Electronic Supplementary Material (ESI) for Dalton Transactions.
This journal is © The Royal Society of Chemistry 2021

Supporting Information

SPAAC iClick: Progress Towards a Bioorthogonal Reaction Incorporating Metal Ions

Yu-Hsuan Shen,[a] Alec M. Esper,[a] Ion Ghiviriga,[a] Khalil A. Abboud,[a] Kirk S. Schanze,[c] Christian Ehm,*[b] Adam S. Veige.*[a]

a. University of Florida, Department of Chemistry, Center for Catalysis, P.O. Box 117200, Gainesville, FL, 32611.
b. Dipartimento di Scienze Chimiche, Università di Napoli Federico II, Via Cintia, 80126 Napoli, Italy.
c. University of Texas at San Antonio, Department of Chemistry, One UTSA Circle, San Antonio, TX 78249.

Corresponding Authors

* E-mail: veige@chem.ufl.edu
E-mail: christian.ehm@unina.it

Table of Contents

1. Syntheses, NMR and X-ray Crystallography Data

1.1 General Considerations

All manipulations were set up under an inert atmosphere using standard Schlenk or glove-box techniques for convenience; however, the compounds are worked up using benchtop technique and are stable in air. Pentane, benzene, and tetrahydrofuran (THF) were degassed by sparging with high purity argon and were dried using a GlassContour drying column. Methanol was dried over anhydrous copper(II) sulfate, distilled and stored over 4 Å molecular sieves; benzene-d_6 (C_6D_6) (Cambridge Isotopes) was dried over sodium benzophenone ketyl, distilled, and stored over 4 Å molecular sieves; chloroform-*d* (Cambridge Isotopes) was dried over calcium hydride, distilled, and stored over 4 Å molecular sieves. Dimethylsulfoxide-d_6 (DMSO-d_6) (Cambridge Isotopes) and acetone was dried over 4 Å molecular sieves for 24 h before use. NMR spectra were recorded on Varian Mercury 300 MHz, Bruker Ascend HD III 400 and 600 MHz spectrometers. 2D NMR spectra were obtained on a Bruker 400 and 600 MHz spectrometer. Chemical shifts are reported in δ (ppm). The values for Ξ (Xi, the frequency ratio of the nucleus) (^{1}H 100.00000%; ^{13}C 25.145020%; ^{15}N 10.132912%) correspond to TMS scale for ^{1}H and ^{13}C and liquid ammonia scale for ^{15}N. ^{31}P{^{1}H} spectra were referenced to an 85% phosphoric acid external standard (0 ppm). ESI-MS analysis was performed at Mass Spectrometry Research and Education Center, at the Chemistry Department at the University of Florida, FL. Elemental analyses were performed at the CENTC Elemental Analysis Facility, Department of Chemistry, University of Rochester and their compositions were determined with a PerkinElmer 2400 Series II Analyzer. X-Ray intensity data were collected at 100 K on a Bruker Dual micro source D8 Venture diffractometer using Mo Kα radiation (λ = 0.71073 Å) and the crystal structure was refined using full-matrix least-squares refinement.[1]

The following were prepared by literature methods: cyclooctyne,[2] [Au(N_3)(PPh_3)] (**Au-N_3**),[3] [W(η^3-allyl)(N_3)(bpy)($CO)_2$] (**W-N_3**),[4] [ReCl(bpy)($CO)_3$],[5] [Ru(N_3)

(Tp)(PPh_3)$_2$] (**Ru-N_3**) [Tp = tris(pyrazolyl)borate],[6] [Pt(N_3)(CH_3)$_3$] **(PtN_3)$_4$**.[7] [Pt(N_3)(CH_3)(P^iPr_3)$_2$] (**Pt(II)-N_3**) was synthesized via a slightly adjusted literature procedure.[8]

Caution! *Azides and azido complexes are potentially explosive. Reactions should be performed only on a small scale until avoiding heat until stability can be verified.*

1.2 Synthesis of $\mathbf{Au_{N1}}$ and $\mathbf{Au_{N2}}$

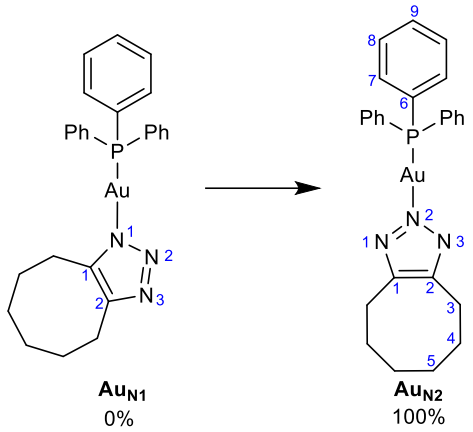

Cyclooctyne (6.5 mg, 0.060 mmol) and **Au-N$_3$** (25.1 mg, 0.0500 mmol) were added into 2 mL of THF. The solution was added to a sealable tube, and the product formation was monitored via ^{31}P NMR spectroscopy. After 48 h, the solvent was removed *in vacuo*, and the precipitate was collected and washed with pentane to give a mixture of $\mathbf{Au_{N1}}$ and $\mathbf{Au_{N2}}$ product. Crystals were grown through pentane diffusion into a THF solution of the triazolate mixture at -25 °C to obtain complex $\mathbf{Au_{N1}}$ as pale-yellow crystals. The complex $\mathbf{Au_{N1}}$ eventually isomerized into 100% $\mathbf{Au_{N2}}$ in solution. 94% Yield of $\mathbf{Au_{N2}}$ (28.7 mg, 0.0471 mmol). ^{1}H NMR (400 MHz, $CDCl_3$): δ 7.50 (m, 15H, C_7-H, C_8-H and C_9-H), 2.90 (dd, $^{3}J_{HH}$ = 3.6 Hz, $^{4}J_{HH}$ = 1.2 Hz, 4H, C_3-H), 1.75 (s, 4H, C_4-H), 1.47 (s, 4H, C_5-H). ^{13}C NMR (101 MHz, $CDCl_3$)): δ 142.7 (s, C_1 and C_2), 134.2 (d, $^{3}J_{CP}$ = 12 Hz, C_8), 132.0 (d, $^{4}J_{CP}$ = 14 Hz, C_9), 129.3 (d, $^{2}J_{CP}$ = 3 Hz, C_7), 128.5 (d, $^{1}J_{CP}$ = 62 Hz, C_6), 28.8 (C_4), 25.7 (C_5), 24.3 (C_3). ^{31}P NMR (121 MHz, $CDCl_3$): δ 33.3. ESI-MS: m/z calculated for $C_{26}H_{27}AuN_3P$ $[M+H]^+$ 610.1686, found 610.1697.

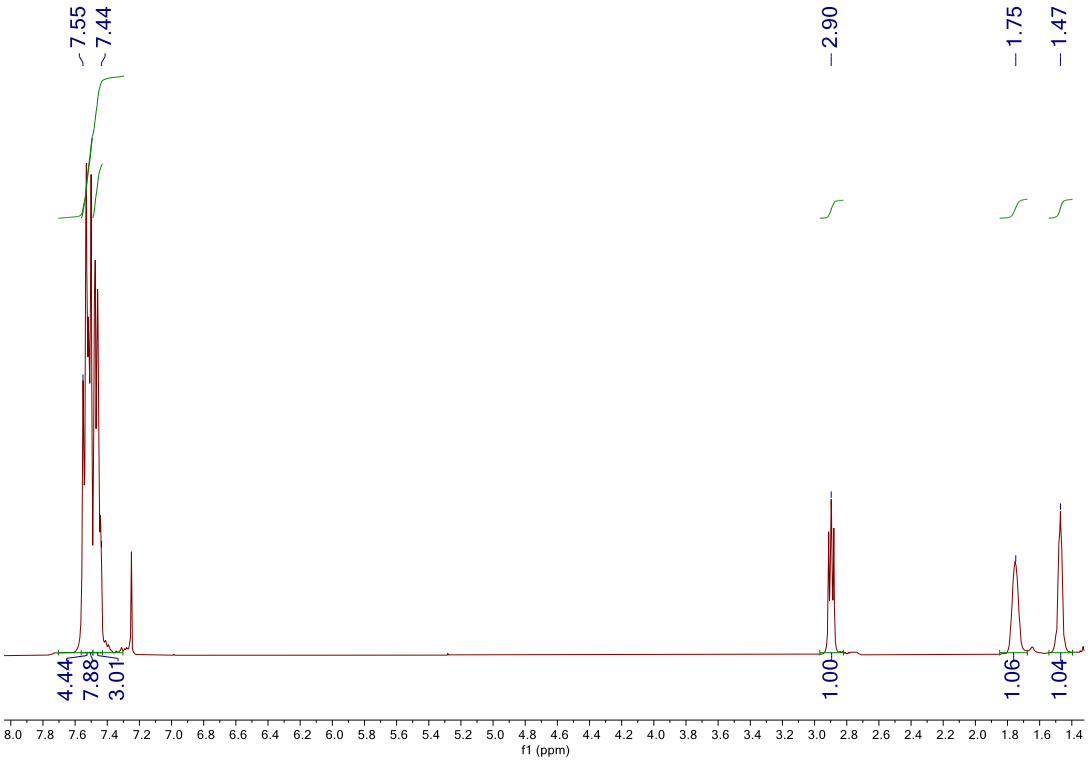

Figure S1. ^{1}H NMR spectrum of **Au_{N2}** ($CDCl_3$, 400 MHz, 25 °C).

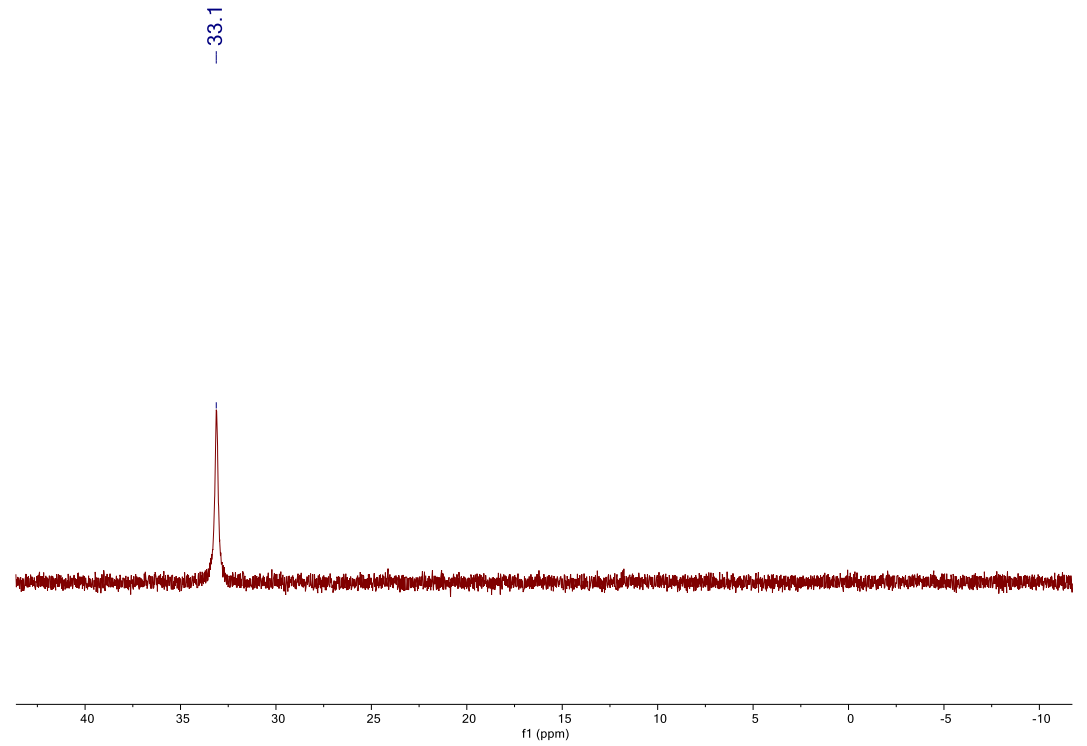

Figure S2. $^{31}P\{^{1}H\}$ NMR spectrum of **Au_{N2}** ($CDCl_3$, 121 MHz, 25 °C).

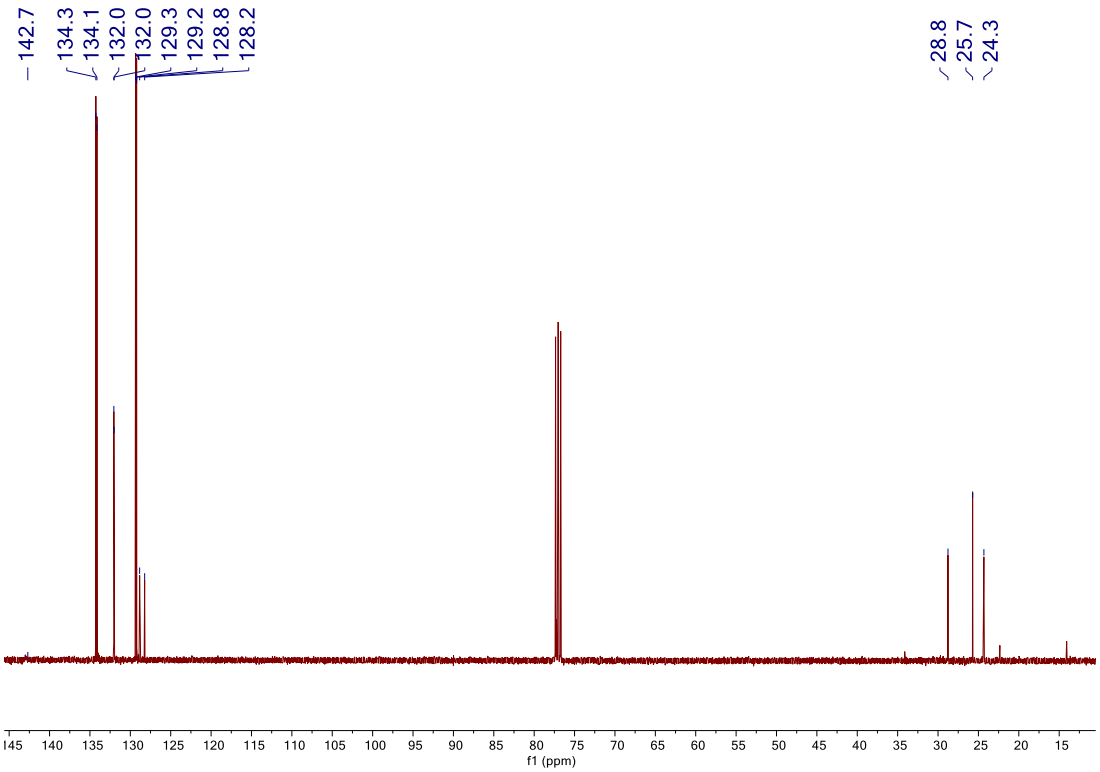

Figure S3. ^{13}C NMR spectrum of **Au_{N2}** ($CDCl_3$, 400 MHz, 25 °C).

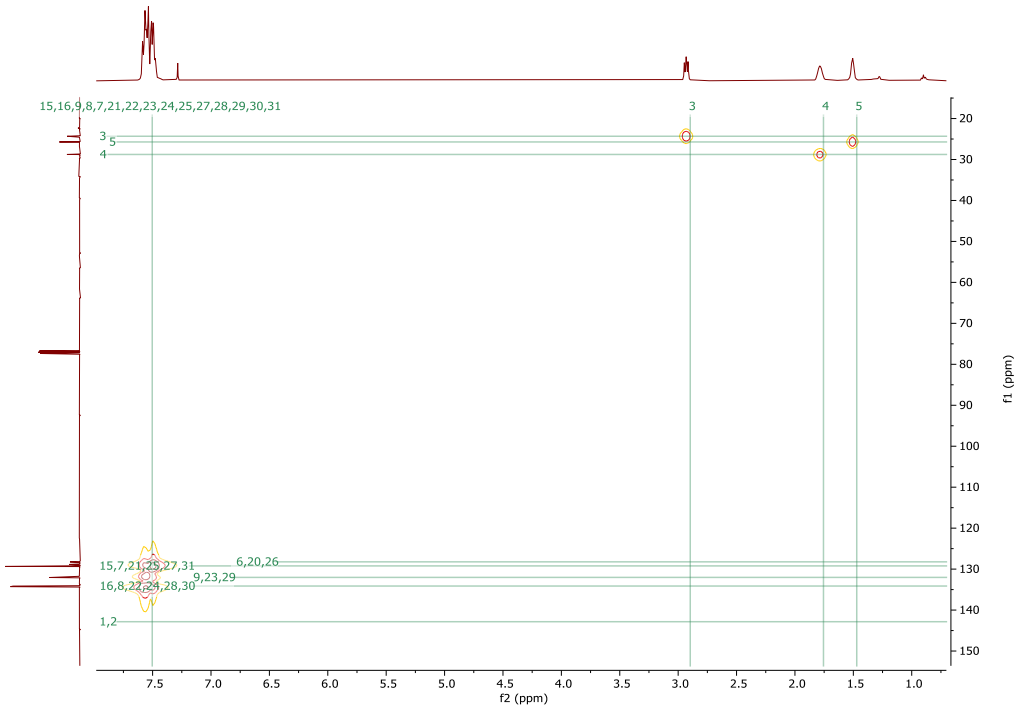

Figure S4. ^{1}H-^{13}C gHSQC spectrum of **Au_{N2}** ($CDCl_3$, 400 MHz, 25 °C).

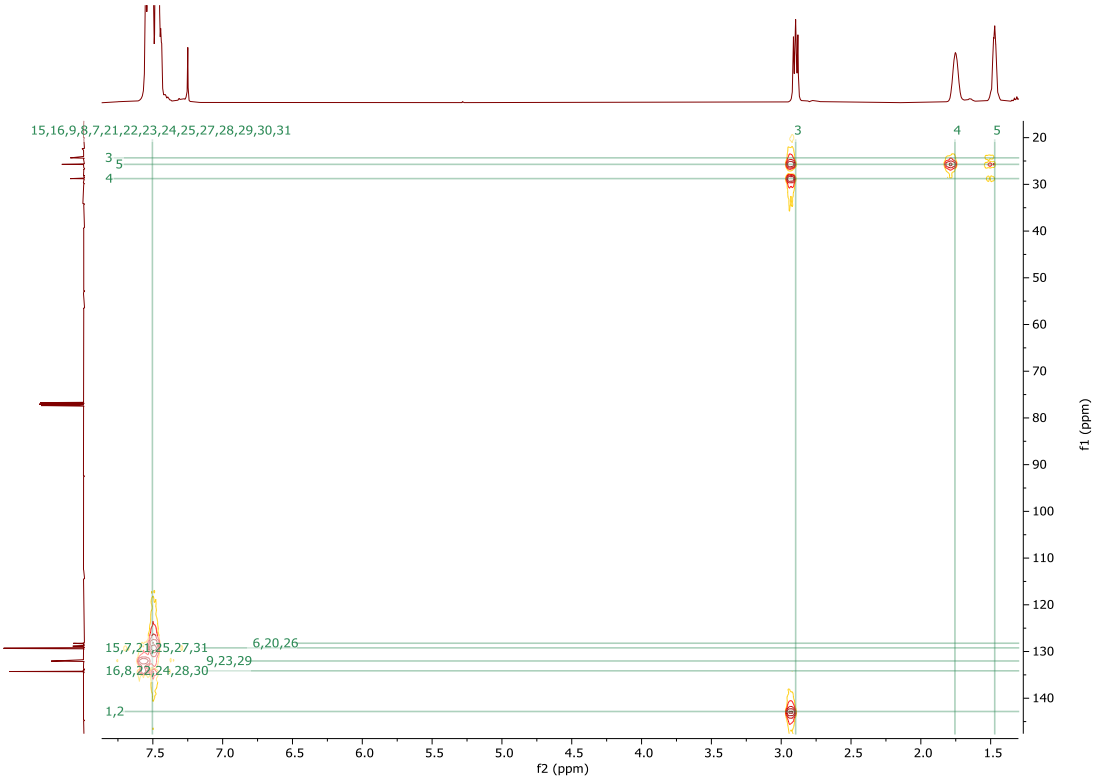

Figure S5. ^{1}H-^{13}C gHBMC spectrum of **Au_{N2}** ($CDCl_3$, 400 MHz, 25 °C).

1.3 X-Ray Crystallography of **Au_{N1}**

X-Ray Intensity data were collected at 100 K on a Bruker Dual micro source D8 Venture diffractometer and PHOTON III detector running APEX3 software package of programs and using Mo Kα radiation (λ = 0.71073 Å). The data frames were integrated, and multi-scan scaling was applied in APEX3. Intrinsic phasing structure solution provided all of the non-H atoms.

The structure was refined using full-matrix least-squares refinement.[1] The non-H atoms were refined with anisotropic displacement parameters and all of the H atoms were calculated in idealized positions and refined riding on their parent atoms. The Au complex has one of the phenyl rings disordered and refined in two parts with their site occupation factors dependently refined to 0.75(1) and 0.25(1), respectively. A major disorder is observed in the C8 ring. Only C41 and C42 are not disordered while the rest of the ring, C43-C48, is disordered and refined in three parts. The site occupation factors of the three parts of C43-C48 disordered parts are dependently refined using SUMP; refined to 0.46(1), 0.24(1 and 0.30(1). In the final cycle of refinement, 8150 reflections (of which

7065 are observed with I > 2 σ (I)) were used to refine 251 parameters and the resulting R_1, wR_2 and S (goodness of fit) were 4.32%, 9.44% and 1.114, respectively. The refinement was carried out by minimizing the wR_2 function using F^2 rather than F values. R_1 is calculated to provide a reference to the conventional R value but its function is not minimized.

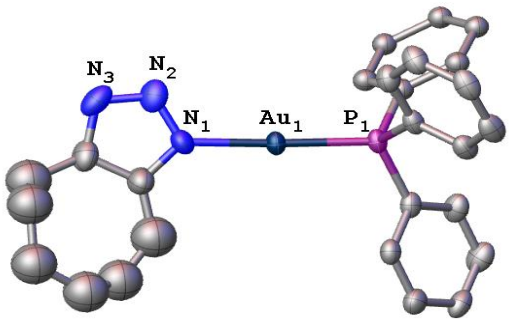

Figure S6. Molecular structure of **Au_{N1}** (Hydrogen atoms removed for clarity).

Table S1. Crystal data and structure refinement for **Au_{N1}**.

CCDC Number	**2068053**
Empirical formula	$C_{26}H_{27}AuN_3P$
Formula weight	609.44
Temperature	100(2) K
Wavelength	0.71073 Å
Crystal system	Monoclinic
Space group	*P* $2_1/n$
Unit cell dimensions	*a* = 12.2089(6) Å, *α*= 90°. *b* = 14.1145(7) Å, *β*= 94.635(2)°. *c* = 13.2833(7) Å, *γ*= 90°.
Volume	2281.5(2) $Å^3$
Z	4
Density (calculated)	1.774 Mg/m^3
Absorption coefficient	6.537 mm^{-1}
F(000)	1192
Crystal size	0.322 x 0.163 x 0.152 mm^3
Theta range for data collection	2.210 to 33.273°.
Index ranges	-18≤h≤18, -21≤k≤20, -19≤l≤20
Reflections collected	70033
Independent reflections	8150 [R(int) = 0.0514]
Completeness to theta = 25.242°	99.6 %
Absorption correction	"multi-scan"
Max. and min. transmission	0.5316 and 0.3341
Refinement method	Full-matrix least-squares on F^2
Data / restraints / parameters	8150 / 104 / 251
Goodness-of-fit on F^2	1.114
Final R indices [I>2sigma(I)]	R_1 = 0.0432, wR_2 = 0.0944 [7065]
R indices (all data)	R_1 = 0.0517, wR_2 = 0.0979
Largest diff. peak and hole	2.575 and -1.610 $e.Å^{-3}$

1.4 Synthesis of **W_{N2}**

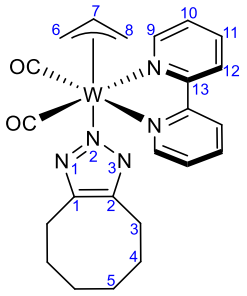

Cyclooctyne (6.5 mg, 0.060 mmol), **$W\text{-}N_3$** (24.0 mg, 0.0500 mmol), and 2 mL of DMSO-d_6 were added to a sealable tube and the product formation was monitored via ^{1}H NMR spectroscopy. After 3 days, the reaction solution was poured into 20 mL benzene and extracted with water several times in order to remove the DMSO. The organic layer was dried over $MgSO_4$, and the solvent was removed *in vacuo* to obtain a hickory-colored powder. Crystals were grown through pentane diffusion into an acetone solution of the triazolate at -25 °C. 59% Yield (17.2 mg, 0.0292 mmol). ^{1}H NMR (400 MHz, DMSO-d_6): δ 8.70 (dd, 2H, $^3J_{HH}$ = 5.5 Hz, $^4J_{HH}$ = 1.6 Hz, C_9-H), 8.59 (d, 2H, $^3J_{HH}$ = 8.2 Hz, C_{12}-H), 8.19 (td, 2H, $^3J_{HH}$ = 7.9 Hz, $^3J_{HH}$ = 1.6 Hz, C_{11}-H), 7.54 (ddd, 2H, $^3J_{HH}$ = 7.2 Hz, $^3J_{HH}$ = 5.4 Hz, $^4J_{HH}$ = 1.2 Hz, C_{10}-H), 2.99 (d, 2H, $^3J_{HH}$ = 6.2 Hz, C_6-H_{syn}, C_8-H_{syn}), 2.32 (m, 4H, C_3-H), 2.21 (tt, 1H, $^3J_{HH}$ = 8.6 Hz, $^3J_{HH}$ = 6.1 Hz, C_7-H), 1.53 (d, 2H, $^3J_{HH}$ = 8.7 Hz, C_6-H_{anti}, C_8-H_{anti}), 1.32 (m, 4H, C_4-H), 1.14 (m, 4H, C_5-H). ^{13}C NMR (101 MHz, DMSO-d_6): δ 223.0 (CO), 158.4 (C_{13}), 151.5 (C_9), 143.0 (C_1, C_2), 138.3 (C_{11}), 127.4 (C_{10}), 123.0 (C_{12}), 66.2 (C_7), 52.6 (C_6, C_8), 27.8 (C_4), 25.5 (C_5), 21.3 (C_3). Anal.: Calc. for $C_{23}H_{25}N_5O_2W$: C, 47.04; H, 4.29; N, 11.92. Found: C, 45.83; H, 4.06; N, 11.49. ESI-MS: m/z calculated for $C_{23}H_{25}N_5O_2W$ $[M+H]^+$ 588.1596, found 588.1566.

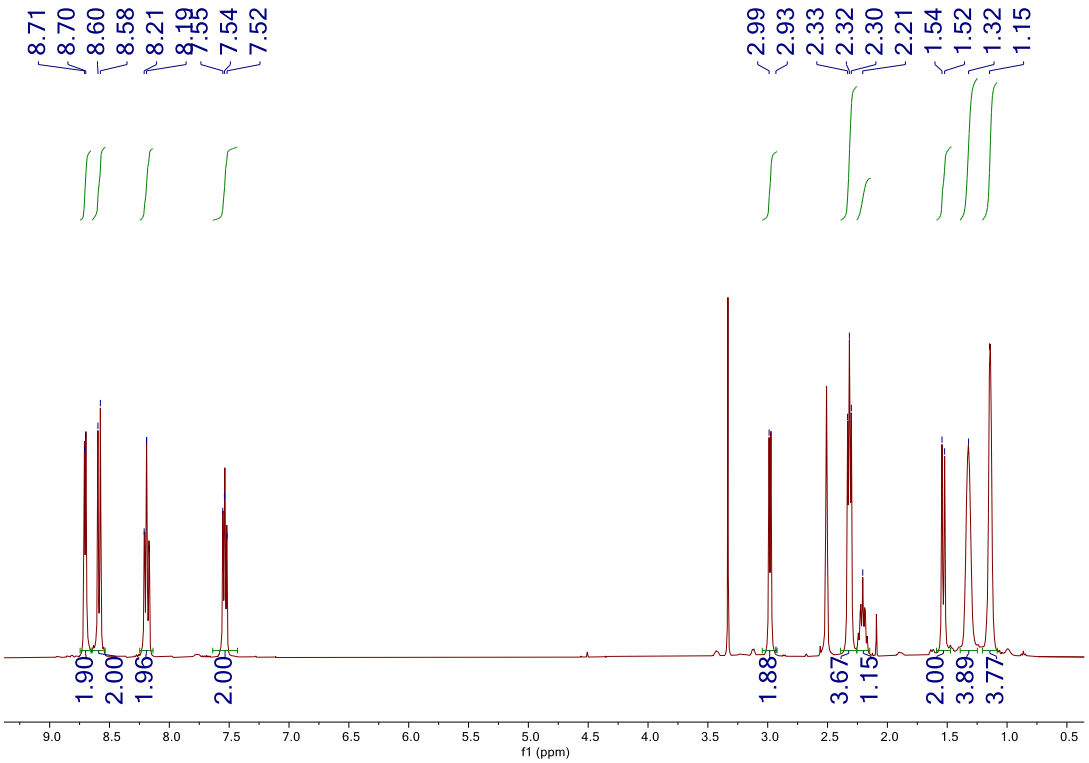

Figure S7. ^{1}H NMR spectrum of $\mathbf{W_{N2}}$ (DMSO-d_6, 400 MHz, 25 °C).

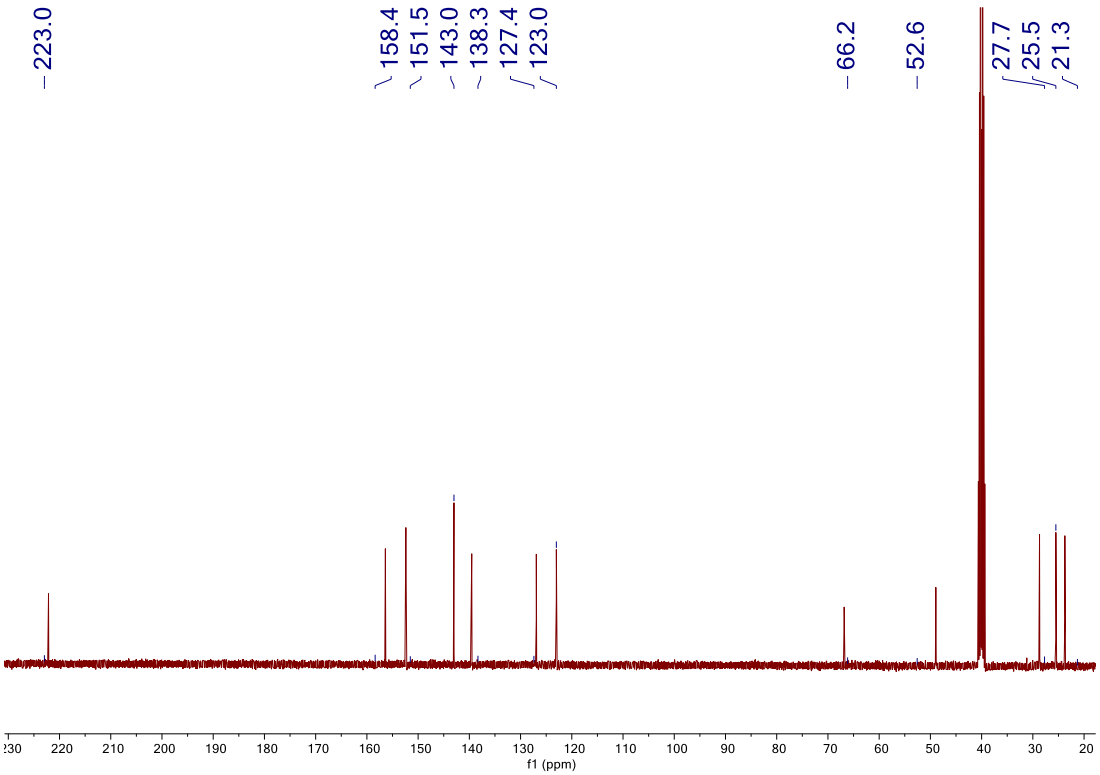

Figure S8. ^{13}C NMR spectrum of $\mathbf{W_{N2}}$ (DMSO-d_6, 101 MHz, 25 °C).

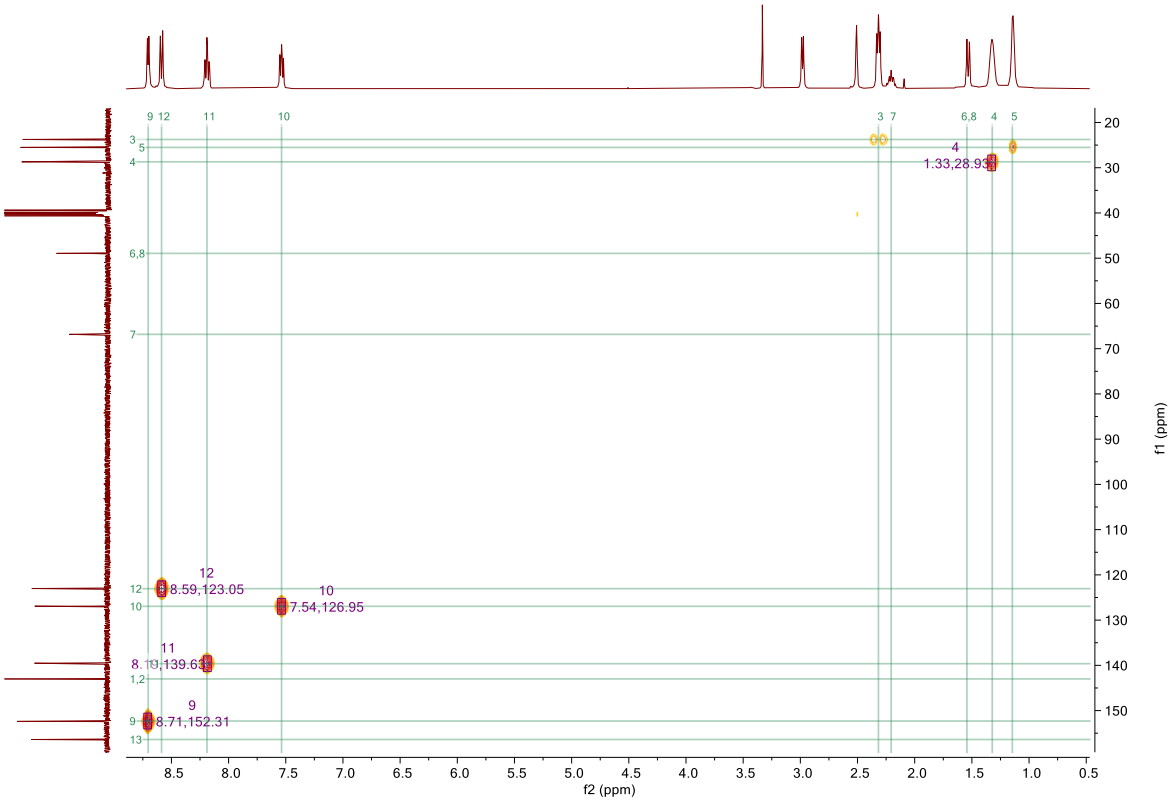

Figure S9. ^{1}H-^{13}C gHSQC spectrum of **W_{N2}** (DMSO-*d*$_6$, 400 MHz, 25 °C).

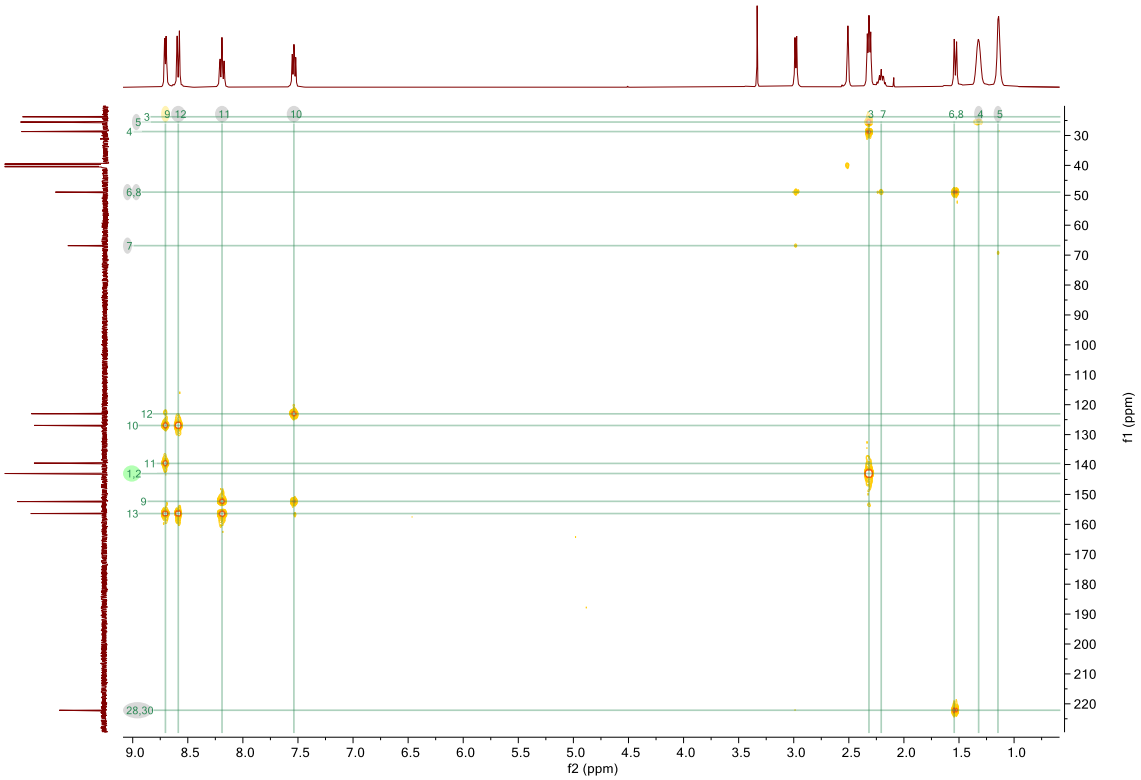

Figure S10. ^{1}H-^{13}C gHMBC spectrum of **W_{N2}** (DMSO-*d*$_6$, 400 MHz, 25 °C).

1.5 X-Ray Crystallography of $\mathbf{W_{N2}}$

X-Ray Intensity data were collected at 100 K on a Bruker Dual micro source D8 Venture diffractometer and PHOTON III detector running APEX3 software package of programs and using Mo Kα radiation (λ = 0.71073 Å). The data frames were integrated, and multi-scan scaling was applied in APEX3. Intrinsic phasing structure solution provided all of the non-H atoms.

The structure was refined using full-matrix least-squares refinement.[1] The non-H atoms were refined with anisotropic displacement parameters and all of the H atoms were calculated in idealized positions and refined riding on their parent atoms. The asymmetric unit consists of the W complex and an acetone solvent molecule. The complex has its oxygen atoms of the carbonyl groups disordered. The bipy group is disordered and refined in two parts. The group of C3-C8 is also disordered and similarly refined in two parts. Finally, the acetone solvent molecule is also disordered and refined in two parts. The structure exhibits all atoms refined anisotropically. In the final cycle of refinement, 8864 reflections (of which 7990 are observed with $I > 2\sigma(I)$) were used to refine 443 parameters and the resulting R_1, wR_2 and S (goodness of fit) were 2.92%, 5.70% and 1.208, respectively. The refinement was carried out by minimizing the wR_2 function using F^2 rather than F values. R_1 is calculated to provide a reference to the conventional R value but its function is not minimized.

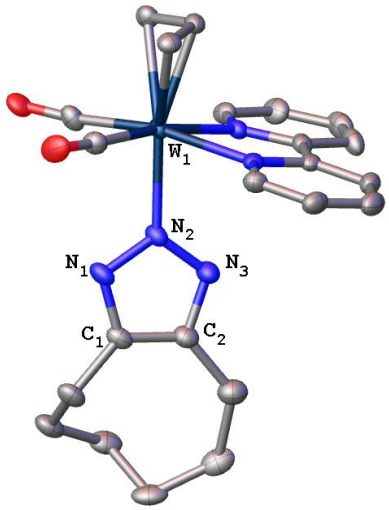

Figure S11. Molecular structure of $\mathbf{W_{N2}}$ (Hydrogen atoms removed for clarity).

Table S2. Crystal data and structure refinement for $\mathbf{W_{N2}}$.

CCDC Number	**2068054**
Empirical formula	$C_{23}H_{25}N_5O_2W$
Formula weight	587.33
Temperature	100(2) K
Wavelength	0.71073 Å
Crystal system	Monoclinic
Space group	$P2_1/n$
Unit cell dimensions	a = 13.915(3) Å, α= 90°. b = 11.0476(18) Å, β= 96.897(6)°. c = 16.410(4) Å, γ= 90°.
Volume	2504.4(9) $Å^3$
Z	4
Density (calculated)	1.558 Mg/m^3
Absorption coefficient	4.639 mm^{-1}
F(000)	1152
Crystal size	0.043 x 0.092x 0.182mm^3
Theta range for data collection	1.815 to 32.763°.
Index ranges	-21≤h≤20, -16≤k≤16, -24≤l≤24
Reflections collected	115078
Independent reflections	8864 [R(int) = 0.0596]
Completeness to theta = 25.242°	100.0 %
Absorption correction	None
Refinement method	Full-matrix least-squares on F^2
Data / restraints / parameters	8864 / 1160 / 443
Goodness-of-fit on F^2	1.208
Final R indices [I>2sigma(I)]	R_1 = 0.0292, wR_2 = 0.0570 [7990]
R indices (all data)	R_1 = 0.0350, wR_2 = 0.0585
Extinction coefficient	n/a
Largest diff. peak and hole	1.149 and -0.891 e.$Å^{-3}$

1.6 Synthesis of **Re-N$_3$**, **Re$_{N1}$**, and **Re$_{N2}$**

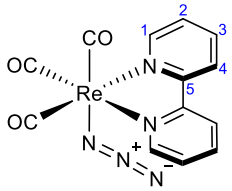

Re-N$_3$

In a degassed mixture of THF:MeOH (1:1 v/v, 6 mL), ReCl(bpy)(CO)$_3$[5] (46.2 mg, 0.100 mmol), silver triflate (77.1 mg, 0.300 mmol) was dissolved and NaN_3 (65.0 mg, 1.00 mmol) was suspended as a heterogeneous mixture and then stirred for a day. After removing all volatiles *in vacuo* a yellow powder was obtained. The powder was washed with distilled water to remove the salts then redissolved in acetone, filtered, and all volatiles removed again to obtain a yellow powder. 59% Yield (27.8 mg, 0.0593 mmol). ^{1}H NMR (400 MHz, DMSO-d_6) δ 9.05 (d, 2H, $^3J_{HH}$ = 5.4 Hz, C_1-H), 8.83 (d, 2H, $^3J_{HH}$ = 8.1 Hz, C_4-H), 8.38 (t, 2H, $^3J_{HH}$ = 6.1 Hz, C_3-H), 7.80 (t, 2H, $^3J_{HH}$ = 7.6 Hz, C_2-H).

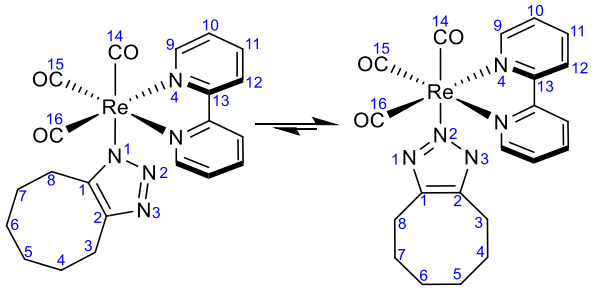

Re$_{N1}$ 34% **Re$_{N2}$** 66%

Cyclooctyne (6.5 mg, 0.060 mmol), **Re-N$_3$** (23.4 mg, 0.0500 mmol), and 2 mL of DMSO-d_6 were added to a sealable tube and the product formation was monitored via ^{1}H NMR spectroscopy. After 8 days, 10 mL of distilled water was poured into the reaction solution and the resulting precipitate was filtered off from the colorless solution, washed with distilled water (10 mL) and pentane (10 mL), and all volatiles were removed *in vacuo* to yield a yellow solid. Crystals were grown through pentane diffusion into an acetone solution of the triazolate at -25 °C. 87% Yield (25.1 mg, 0.0435 mmol). ^{1}H NMR (600 MHz, DMSO-d_6) δ major **Re$_{N2}$** isomer: 9.06 (dd, 2H, $^3J_{HH}$ = 5.4 Hz, $^4J_{HH}$ = 1.5 Hz, C_9-H), 8.62 (d, 2H, $^3J_{HH}$ = 8.1 Hz, C_{12}-H), 8.27 (td, 2H, $^3J_{HH}$ = 7.9 Hz, $^3J_{HH}$ = 1.6 Hz, C_{11}-H), 7.71 (ddd, 2H, $^3J_{HH}$ = 7.2 Hz, $^3J_{HH}$ = 5.5 Hz, $^4J_{HH}$ = 1.4 Hz, C_{10}-H), 2.33 (m, 4H, C_3-H, C_8-H), 1.32 (m, 4H, C_4-H, C_7-H), 1.11 (p, $^3J_{HH}$ = 2.6 Hz, 4H, C_5-H, C_6-H); δ minor **Re$_{N1}$** isomer: 9.04

(dd, *J* = 5.4, 1.5 Hz, 2H, C_9-H), 8.72 (d, 2H, *J* = 8.1 Hz, C_{12}-H), 8.31 (td, 2H, *J* = 7.9, 1.6 Hz, C_{11}-H), 7.71 (ddd, 2H, *J* = 7.2, 5.5, 1.4 Hz, C_{10}-H), 2.76 (m, 2H, C_8-H), 2.50 (m, 2H, C_3-H), 1.51 (p, *J* = 6.4 Hz, 2H, C_7-H), 1.43 (d, *J* = 6.7 Hz, 2H, C_4-H), 1.28 (t, *J* = 5.6 Hz, 2H, C_6-H), 1.19 (d, *J* = 5.9 Hz, 2H, C_5-H). ^{13}C NMR (151 MHz, DMSO-*d*$_6$): δ major **Re$_{N2}$** isomer: 198.9 (C_{15}, C_{16}), 195.7 (C_{14}), 156.2 (C_{13}), 153.7 (C_9), 142.6 (C_1, C_2), 140.5 (C_{11}), 128.0 (C_{10}), 124.0 (C_{12}), 28.9 (C_4, C_7), 25.5 (C_5, C_6), 23.8 (C_3, C_8); δ minor **Re$_{N1}$** isomer: 198.3 (C_{15}, C_{16}), 195.7 (C_{14}), 156.6 (C_{13}), 153.7 (C_9), 141.4 (C_1), 140.7 (C_{11}), 140.6 (C_2), 128.2 (C_{10}), 124.3 (C_{12}), 29.4 (C_4), 28.6 (C_7), 26.0 (C_6), 25.4 (C_5), 24.9 (C_8), 24.3 (C_3). ^{15}N NMR (61 MHz, DMSO-*d*$_6$): δ major **Re$_{N2}$** isomer: 349.8 (N_1, N_3), 246.7 (N_4); δ minor **Re$_{N1}$** isomer: 351.9 (N_3), 267.1 (N_1), 245.50 (N_4). ESI-MS: m/z calculated for $C_{21}H_{20}N_5O_3Re$ $[M+H]^+$ 578.1202, found 578.1203.

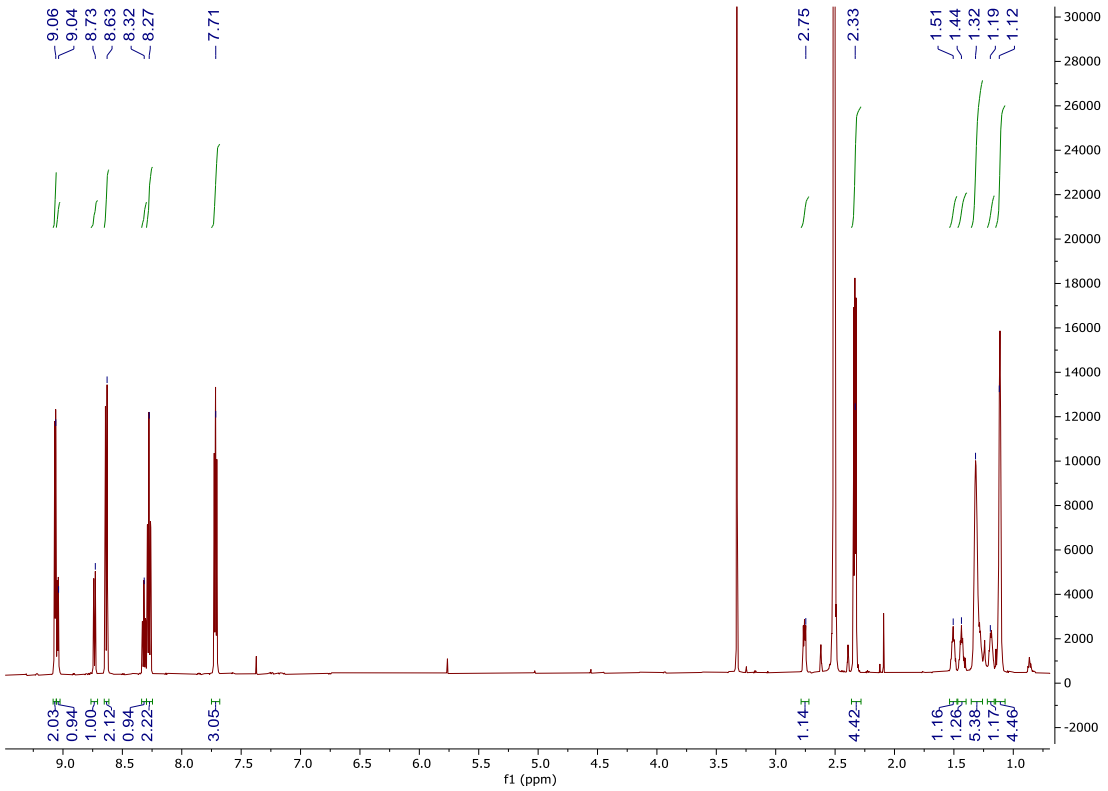

Figure S12. ^{1}H NMR spectrum of **Re$_{N1}$** and **Re$_{N2}$** (DMSO-*d*$_6$, 600 MHz, 25 °C).

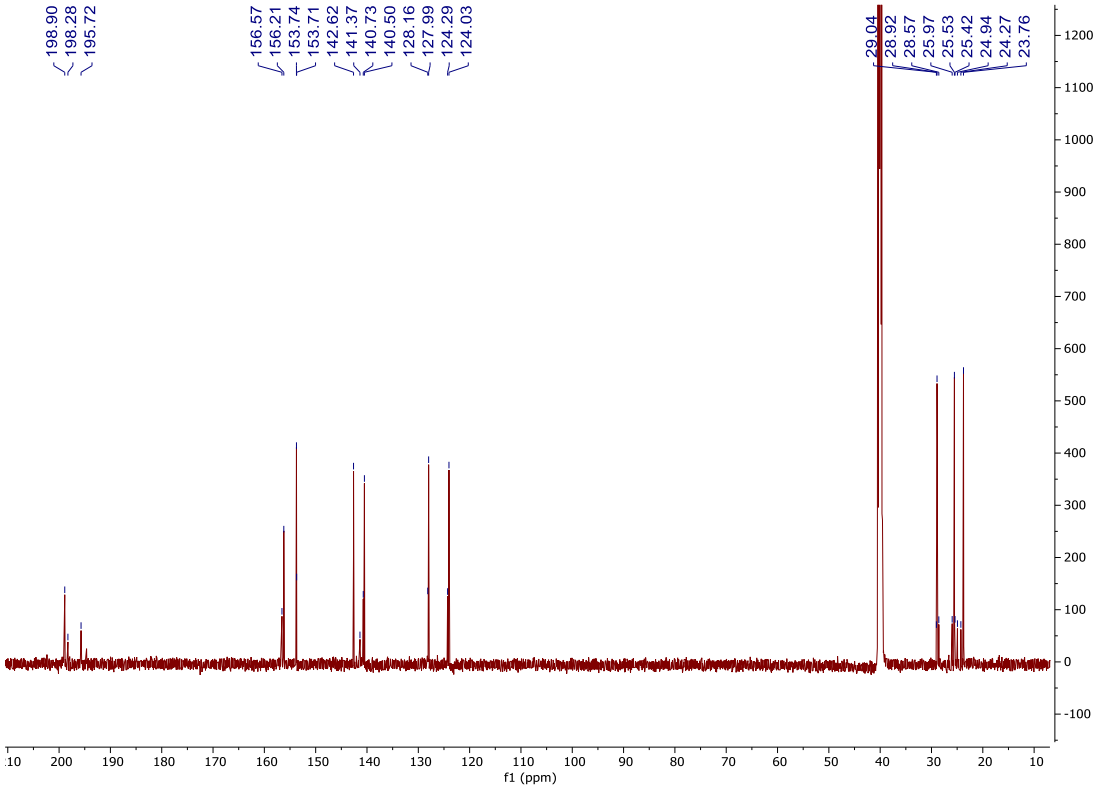

Figure S13. ^{13}C NMR spectrum of **Re$_{N1}$** and **Re$_{N2}$** (DMSO-*d*$_6$, 151 MHz, 25 °C).

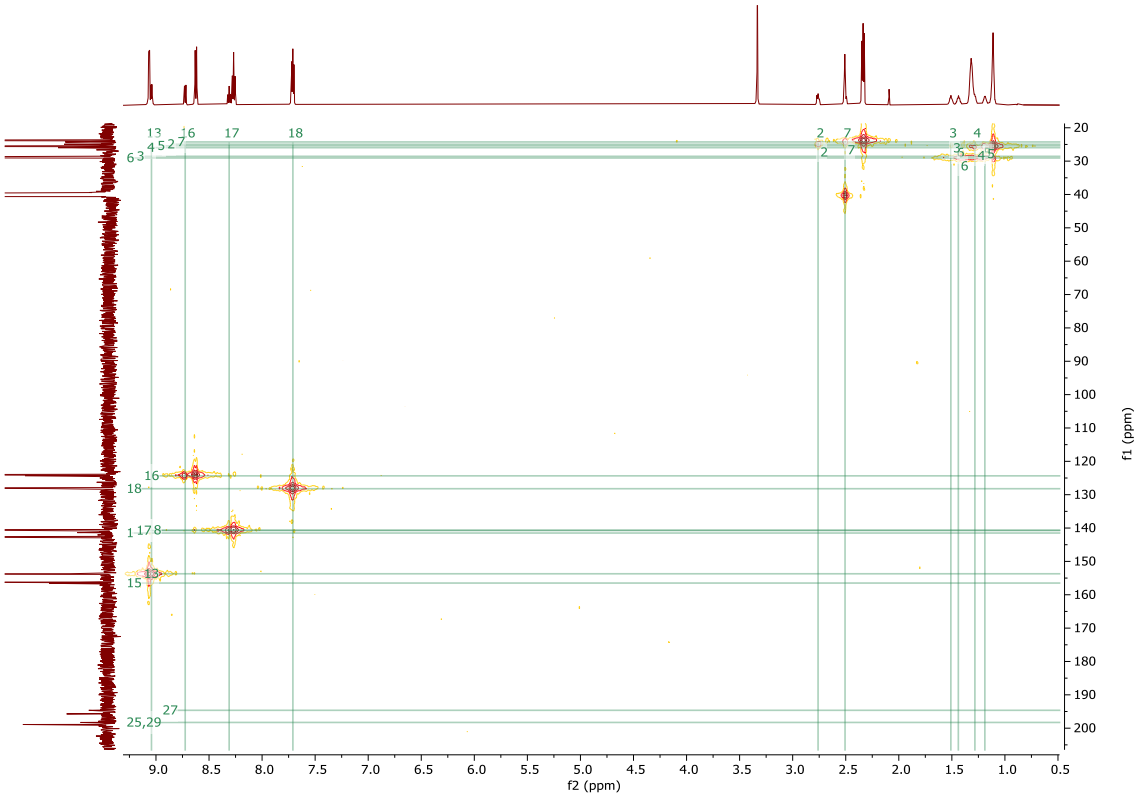

Figure S14. ^{1}H-^{13}C gHSQC spectrum of **Re_{N1}** and **Re_{N2}** (DMSO-d_6, 600 MHz, 25 °C).

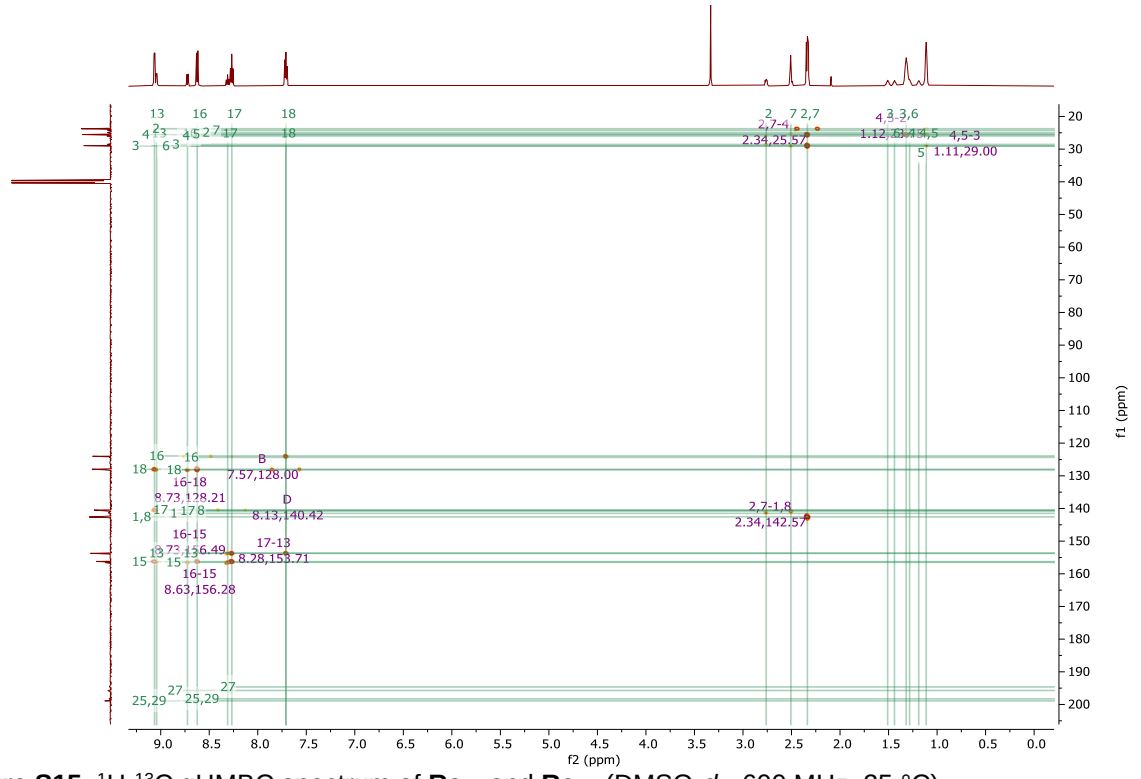

Figure S15. ^{1}H-^{13}C gHMBC spectrum of **Re_{N1}** and **Re_{N2}** (DMSO-d_6, 600 MHz, 25 °C).

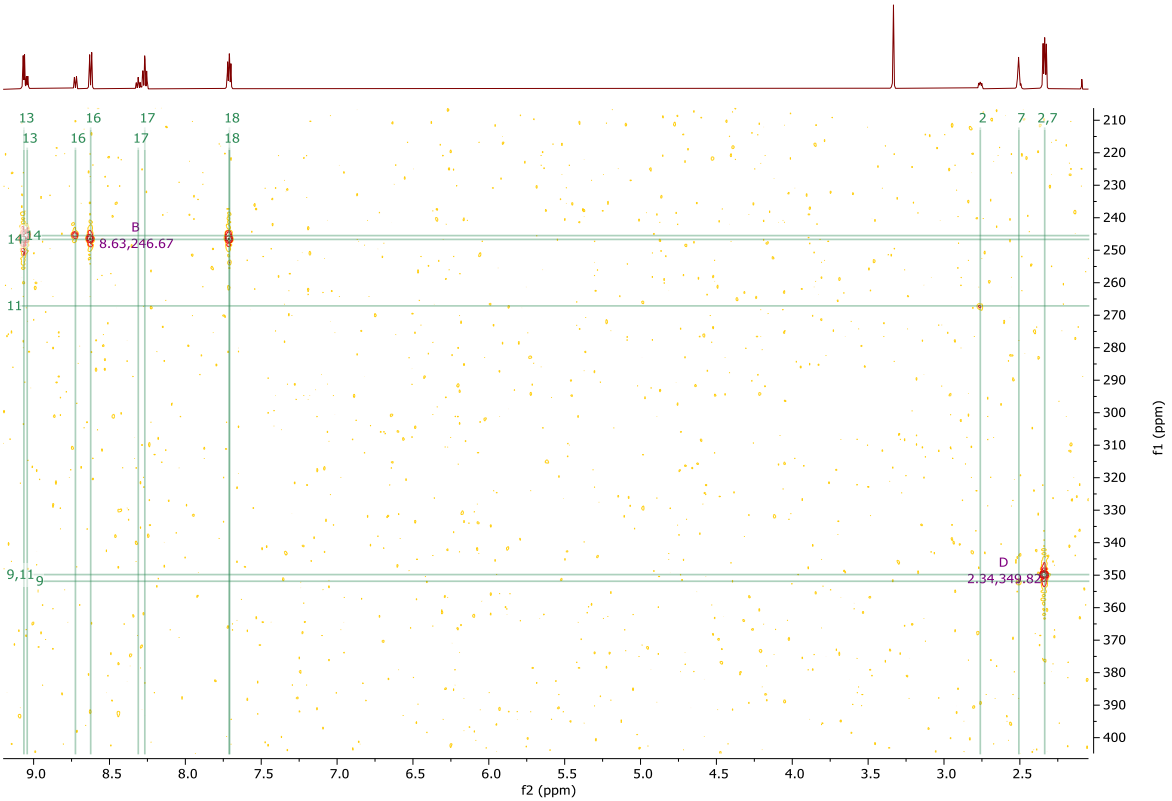

Figure S16. ^{1}H-^{15}N gHMBC spectrum of **Re_{N1}** and **Re_{N2}** (DMSO-d_6, 600 MHz, 25 °C).

1.7 X-Ray Crystallography of **Re_{N2}**

X-Ray Intensity data were collected at 100 K on a Bruker Dual micro source D8 Venture diffractometer and PHOTON III detector running APEX3 software package of programs and using Mo Kα radiation (λ = 0.71073 Å). The data frames were integrated and multi-scan scaling was applied in APEX3. Intrinsic phasing structure solution provided the All of the non-H atoms.

The structure was refined using full-matrix least-squares.[1] The non-H atoms were refined with anisotropic displacement parameters and all of the H atoms were calculated in idealized positions and refined riding on their parent atoms. One oxygen atom of a carbonyl ligand is disordered and refined in two parts with their site occupations factors dependently refined. The C3-C8 part of the C8 ring is also disordered and also refined in two parts with their site occupation factors dependently refined. The equivalent bonds in the –C3-C8- part of the ring were constrained to stay geometrically equivalent using the SADI command lines. In the final cycle of refinement, 8592 reflections (of which 7613 are observed with I > 2σ(I)) were used to refine 331 parameters and the resulting R_1, wR_2 and S (goodness of fit) were 2.62%, 5.78% and 1.088, respectively. The refinement was carried out by minimizing the wR_2 function using F^2 rather than F values. R_1 is calculated to provide a reference to the conventional R value but its function is not minimized.

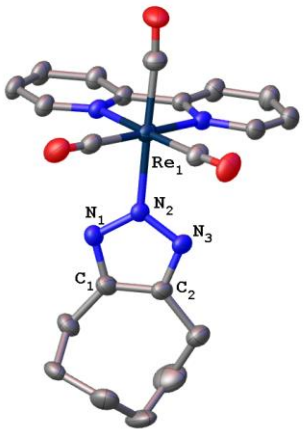

Figure S17. Molecular structure of **Re_{N2}** (All hydrogen atoms removed for clarity).

Table S3. Crystal data and structure refinement for **Re_{N2}**.

CCDC Number	**2068055**
Empirical formula	$C_{21}H_{20}N_5O_3Re$
Formula weight	576.62
Temperature	100(2) K
Wavelength	0.71073 Å
Crystal system	Triclinic
Space group	*P*-1
Unit cell dimensions	*a* = 10.099(7) Å, *α*= 77.240(15)°. *b* = 10.839(6) Å, *β*= 72.021(16)°. *c* = 11.962(9) Å, *γ* = 85.85(2)°.
Volume	1214.7(14) $Å^3$
Z	2
Density (calculated)	1.576 Mg/m^3
Absorption coefficient	5.030 mm^{-1}
F(000)	560
Crystal size	0.343 x 0.070 x 0.034 mm^3
Theta range for data collection	1.926 to 33.181°.
Index ranges	-15≤h≤15, -16≤k≤16, -17≤l≤18
Reflections collected	77811
Independent reflections	8592 [R(int) = 0.0451]
Completeness to theta = 25.242°	100.0 %
Absorption correction	"Multi-Scan"
Refinement method	Full-matrix least-squares on F^2
Data / restraints / parameters	8592 / 660 / 331
Goodness-of-fit on F^2	1.088
Final R indices [I>2sigma(I)]	R_1 = 0.0262, wR_2 = 0.0578 [7613]
R indices (all data)	R_1 = 0.0328, wR_2 = 0.0607
Extinction coefficient	n/a
Largest diff. peak and hole	2.374 and -1.877 $e.Å^{-3}$

1.8 Synthesis of **Pt(II)-N_3**, **Pt(IV)-N_3**, and **Pt(IV)$_{N2}$**

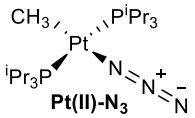

Pt(II)-N_3

$Pt(CH_3)(P^iPr_3)_2(N_3)$ (**Pt(II)-N_3**) was synthesized via a slightly adjusted literature procedure.[8] $Pt(CH_3)_3(N_3)$ (**$(PtN_3)_4$**)[7] (141.1 mg, 0.5000 mmol) and $P(P^iPr_3)_3$ (192.3 mg, 1.200 mmol) were dissolved in 5 mL toluene and heated at 80 °C for 2 h. The reaction solution was filtered and all volatiles removed *in vacuo* to obtain a white powder. The powder was further washed with pentane, then all volatiles were removed again to yield a white powder. 68% Yield (193.4 mg, 0.3377 mmol).

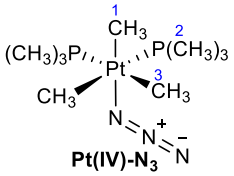

Pt(IV)-N_3

$(PtN_3)_4$[7] (141.1 mg, 0.5000 mmol) and $P(CH_3)_3$ (91.2 mg, 1.20 mmol) were dissolved in toluene (5 mL) and heated at 80 °C for 2 h. All volatiles were removed *in vacuo* to obtain a white powder. The powder was further washed with pentane then all volatiles were removed again to yield a white solid. Crystals were grown through pentane diffusion into a toluene solution of the azide at -25 °C. 60% Yield (130.3 mg, 0.2993 mmol). ^{1}H NMR (400 MHz, C_6D_6): δ 1.09 (m, 6H, C_3-H), 0.78 (m, 18H, C_2-H), 0.29 (tt, 3H, $^2J_{HPt}$ = 67.8 Hz, $^3J_{HP}$ = 7.8 Hz, C_1-H). ^{13}C NMR (101 MHz, C_6D_6): δ 11.2 (m, C_2), 6.7 (m, $^1J_{CPt}$ = 513 Hz, $^2J_{CPtrans}$ = 125 Hz, $^2J_{CPcis}$ = 8 Hz, C_3), -15.1 (tt, $^1J_{CPt}$ = 615 Hz, $^2J_{CP}$ = 3 Hz, C_1). ^{31}P NMR (121 MHz, C_6D_6): δ -42.3. ESI-MS: m/z calculated for $C_9H_{27}N_3P_2Pt$ $[M+Na]^+$ 457.1226, found 457.1209.

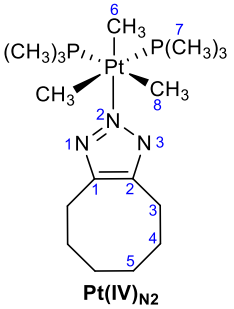

Pt(IV)$_{N2}$

Cyclooctyne (32.4 mg, 0.300 mmol), **Pt(IV)-N_3** (108.6 mg, 0.2500 mmol), and 2 mL of C_6D_6 were added to a sealable tube. The tube was heated at 50 °C and the product

formation was monitored via ^{31}P NMR spectroscopy. After 5 days, the reaction solution was filtered and all volatiles removed to obtain a white powder. The powder was further washed with cold pentane several times, then all volatiles were removed to yield a white solid. Colorless crystals were grown through cooling the pentane solution of the triazolate at -25 °C. 13% Yield (17.6 mg, 0.0324 mmol). ^{1}H NMR (400 MHz, C_6D_6): δ 3.01 (t, $^{3}J_{HH}$ = 4 Hz, 4H, C_3-H), 1.75 (m, 4H, C_4-H), 1.48 (m, 4H, C_5-H), 1.38 (m, 6H, C_8-H), 0.93 (m, 18H, C_7-H), 0.33 (tt, 3H, $^{2}J_{HPt}$ = 67.8 Hz, $^{3}J_{HP}$ = 7.8 Hz, C_6-H). ^{13}C NMR (101 MHz, C_6D_6): δ 142.7 (C_1 and C_2), 29.9 (C_4), 26.0 (C_5), 24.4 (C_3), 12.0 (m, C_7), 7.7 (m, $^{1}J_{CPt}$ = 513 Hz, $^{2}J_{CPtrans}$ = 125 Hz, $^{2}J_{CPcis}$ = 8 Hz, C_8), -17.8 (t, $^{1}J_{CPt}$ = 615 Hz, C_6). ^{31}P NMR (121 MHz, C_6D_6): δ -42.0. Anal.: Calc. for $C_{17}H_{39}N_3P_2Pt$: C, 37.63; H, 7.25; N, 7.75. Found: C, 37.79; H, 7.23; N, 7.66. ESI-MS: m/z calculated for $C_{17}H_{39}N_3P_2Pt$ $[M+H]^+$ 543.2345, found 543.2389.

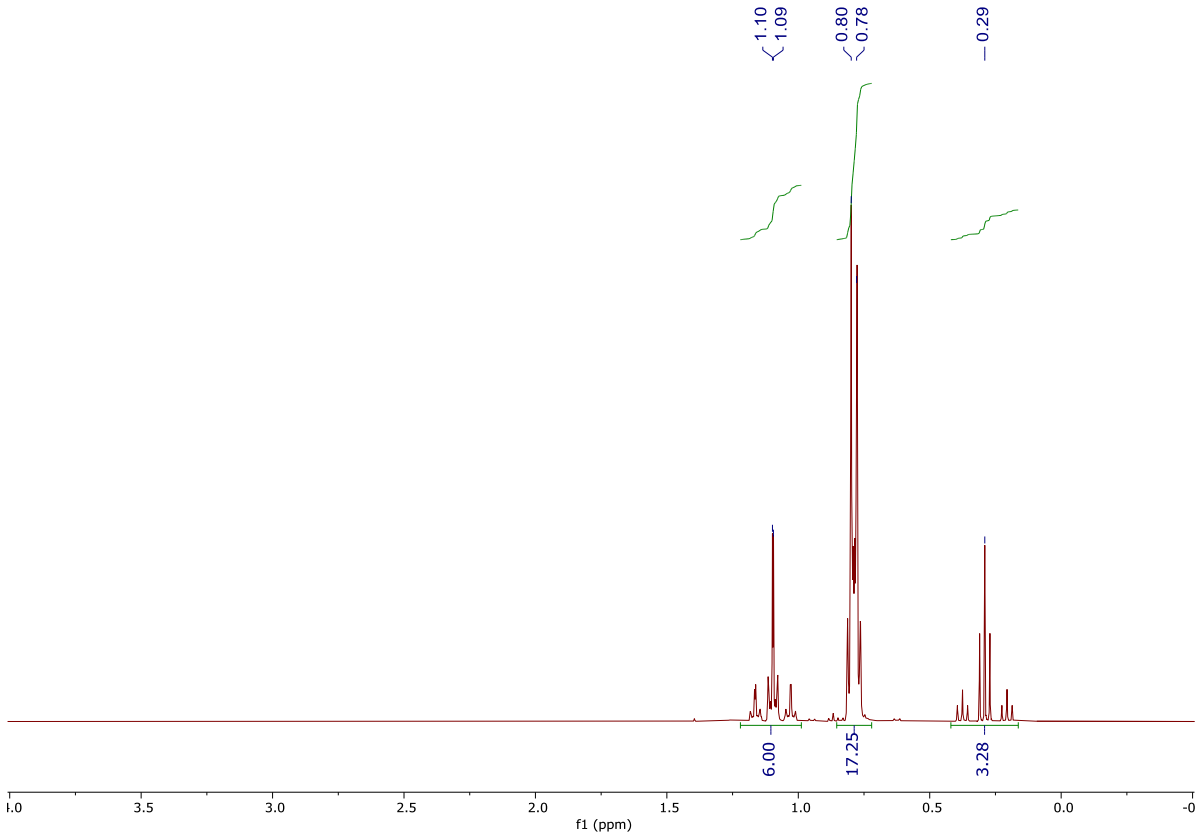

Figure S18. ^{1}H NMR spectrum of **Pt(IV)-N_3** (C_6D_6, 400 MHz, 25 °C).

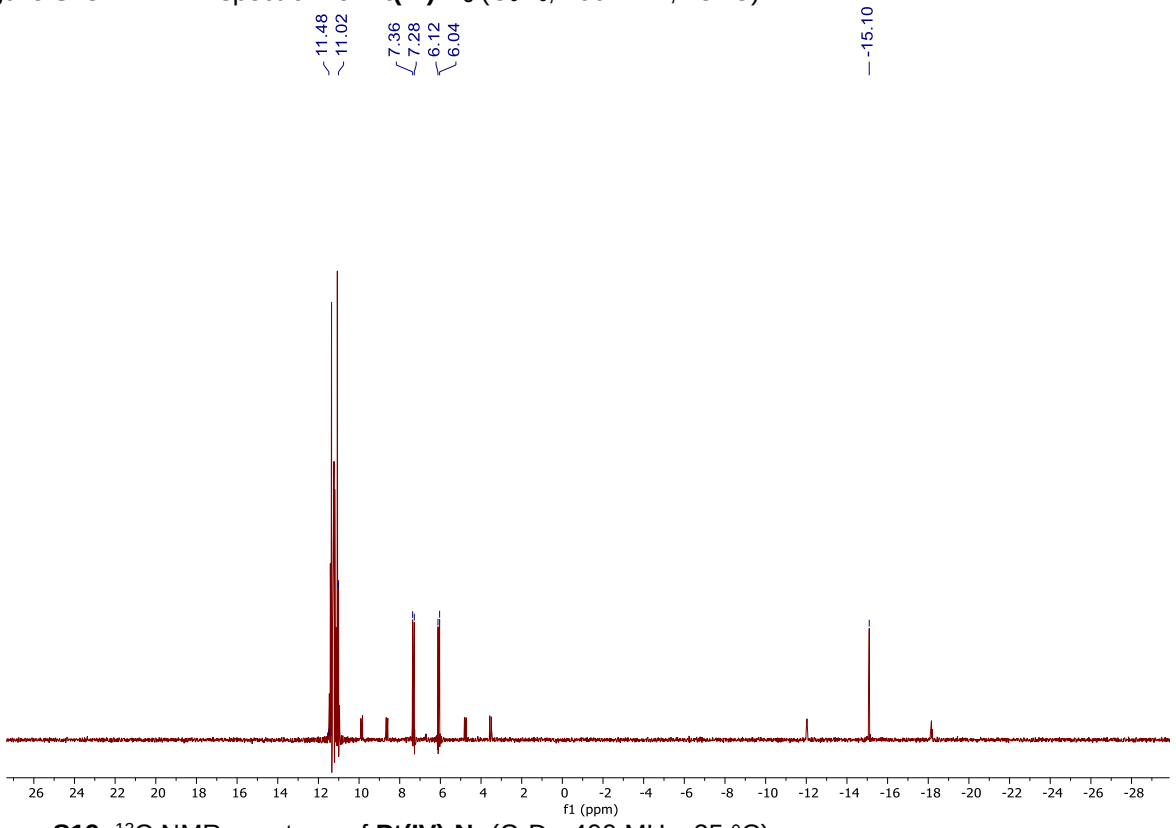

Figure S19. ^{13}C NMR spectrum of **Pt(IV)-N_3** (C_6D_6, 400 MHz, 25 °C).

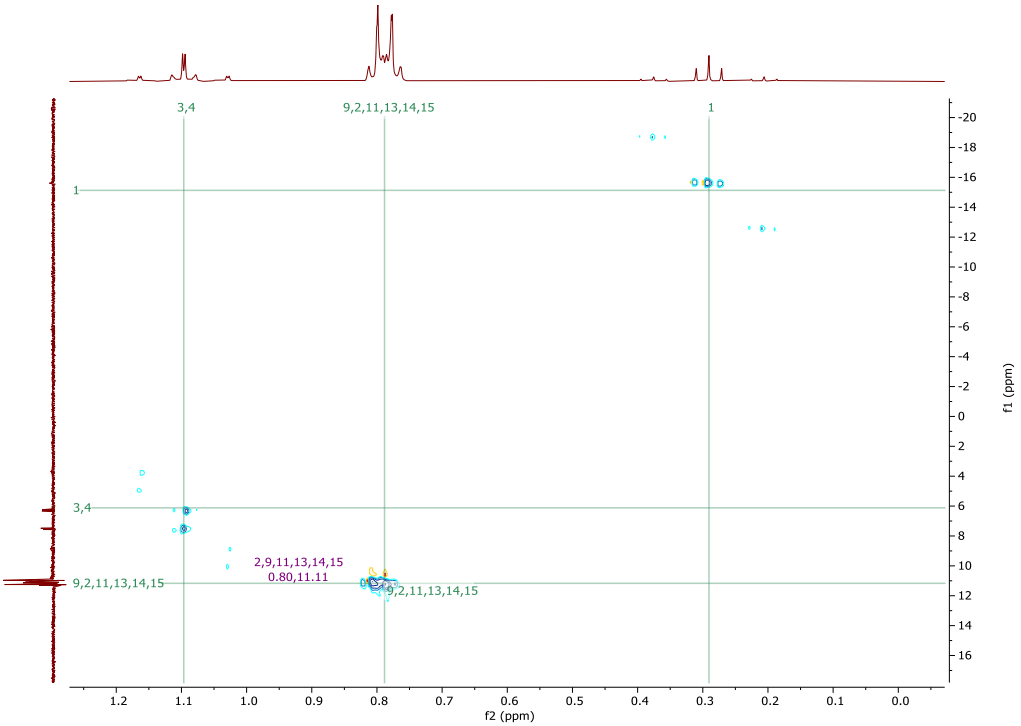

Figure S20. ^{1}H-^{13}C gHSQC spectrum of **Pt(IV)-N_3** (C_6D_6, 400 MHz, 25 °C).

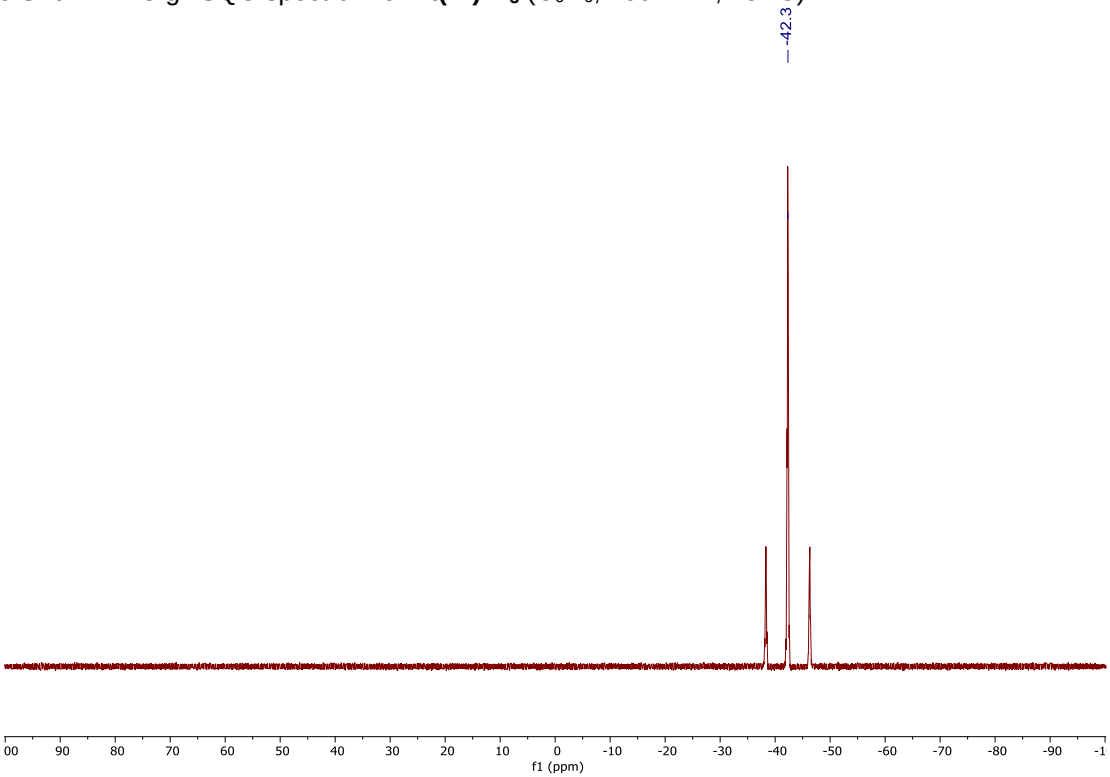

Figure S21. $^{31}P\{^{1}H\}$ NMR spectrum of **Pt(IV)-N_3** (C_6D_6, 162 MHz, 25 °C).

1.9 X-Ray Crystallography of **Pt(IV)-N_3**

X-Ray Intensity data were collected at 100 K on a Bruker Dual micro source D8 Venture diffractometer and PHOTON III detector running APEX3 software package of programs and using Mo Kα radiation (λ = 0.71073 Å). The data frames were integrated, and multi-scan scaling was applied in APEX3. Intrinsic phasing structure solution provided all of the non-H atoms.

The structure was refined using full-matrix least-squares refinement.[1] The non-H atoms were refined with anisotropic displacement parameters and all of the H atoms were calculated in idealized positions and refined riding on their parent atoms. In the final cycle of refinement, 4710 reflections (of which 4398 are observed with I > 2σ(I)) were used to refine 145 parameters and the resulting R_1, wR_2 and S (goodness of fit) were 2.19%, 4.78% and 1.200, respectively. The refinement was carried out by minimizing the wR_2 function using F^2 rather than F values. R_1 is calculated to provide a reference to the conventional R value but its function is not minimized.

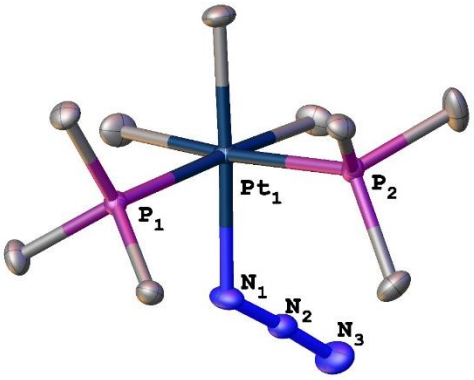

Figure S22. Molecular structure of **Pt(IV)-N_3** (All hydrogen atoms removed for clarity).

Table S4. Crystal data and structure refinement for **Pt(IV)-N_3**.

CCDC Number	**2068056**
Empirical formula	$C_9H_{27}N_3P_2Pt$
Formula weight	434.36
Temperature	100(2) K
Wavelength	0.71073 Å
Crystal system	Orthorhombic
Space group	*Pbca*
Unit cell dimensions	*a* = 13.7352(9) Å, *α*= 90°. *b* = 11.7608(7) Å, *β*= 90°. *c* = 19.1917(13) Å, *γ*= 90°.
Volume	3100.2(3) $Å^3$
Z	8
Density (calculated)	1.861 Mg/m^3
Absorption coefficient	9.238 mm^{-1}
F(000)	1680
Crystal size	0.170 x 0.130 x 0.093 mm^3
Theta range for data collection	2.122 to 30.529°.
Index ranges	-19≤h≤19, -16≤k≤16, -27≤l≤27
Reflections collected	51254
Independent reflections	4710 [R(int) = 0.0647]
Completeness to theta = 25.242°	98.8 %
Absorption correction	multi-scan
Refinement method	Full-matrix least-squares on F^2
Data / restraints / parameters	4710 / 0 / 145
Goodness-of-fit on F^2	1.200
Final R indices [I>2sigma(I)]	R_1 = 0.0219, wR_2 = 0.0478 [4398]
R indices (all data)	R_1 = 0.0237, wR_2 = 0.0485
Extinction coefficient	n/a
Largest diff. peak and hole	1.175 and -1.577 $e.Å^{-3}$

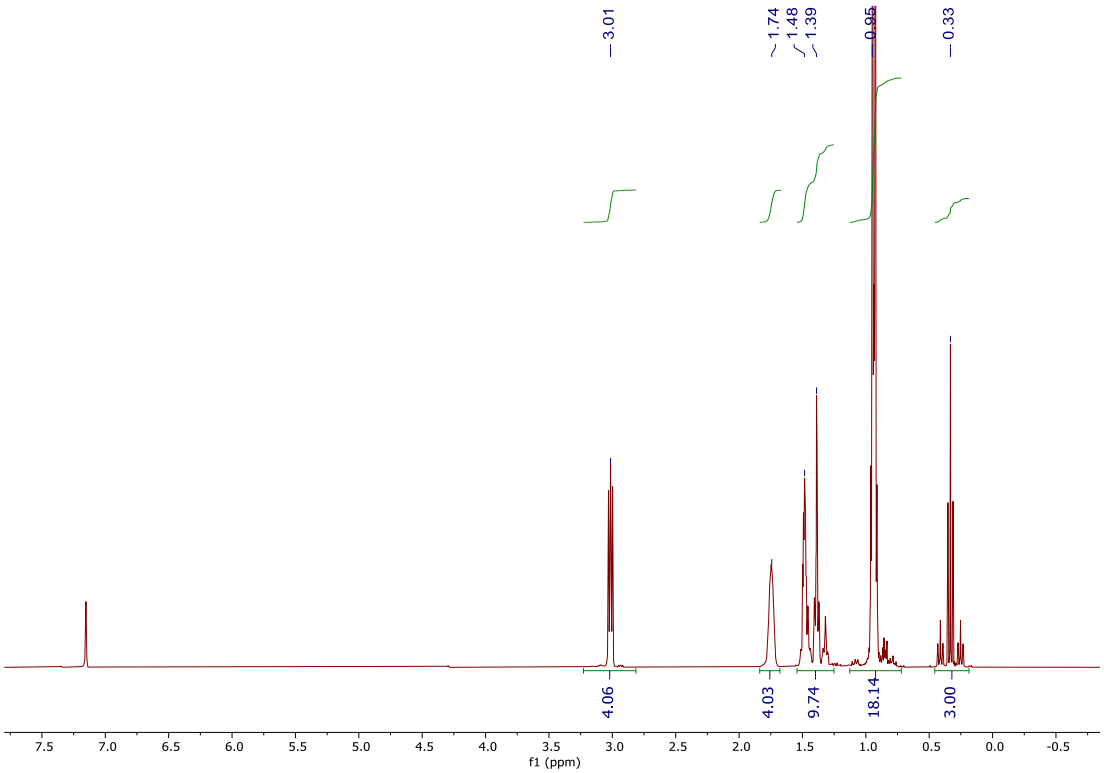

Figure S23. ^{1}H NMR spectrum of **Pt(IV)$_{N2}$** (C_6D_6, 400 MHz, 25 °C).

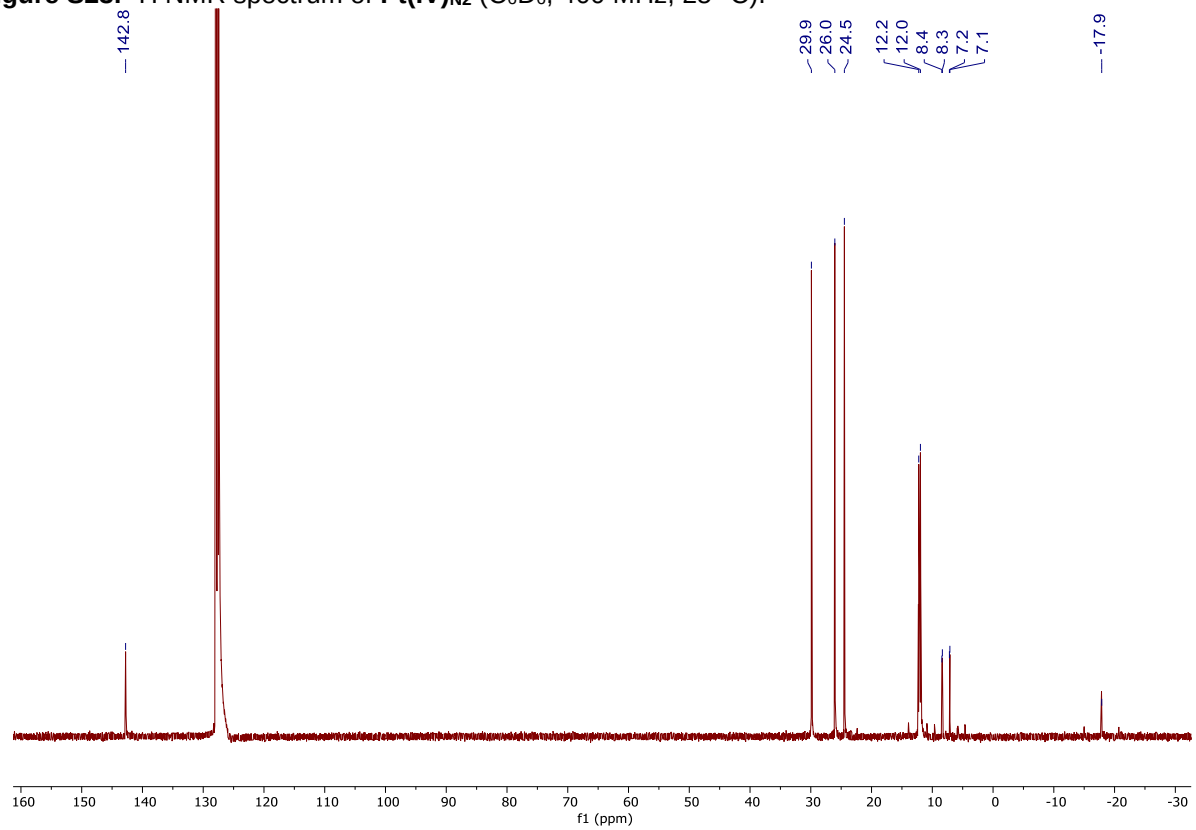

Figure S24. ^{13}C NMR spectrum of **Pt(IV)$_{N2}$** (C_6D_6, 400 MHz, 25 °C).

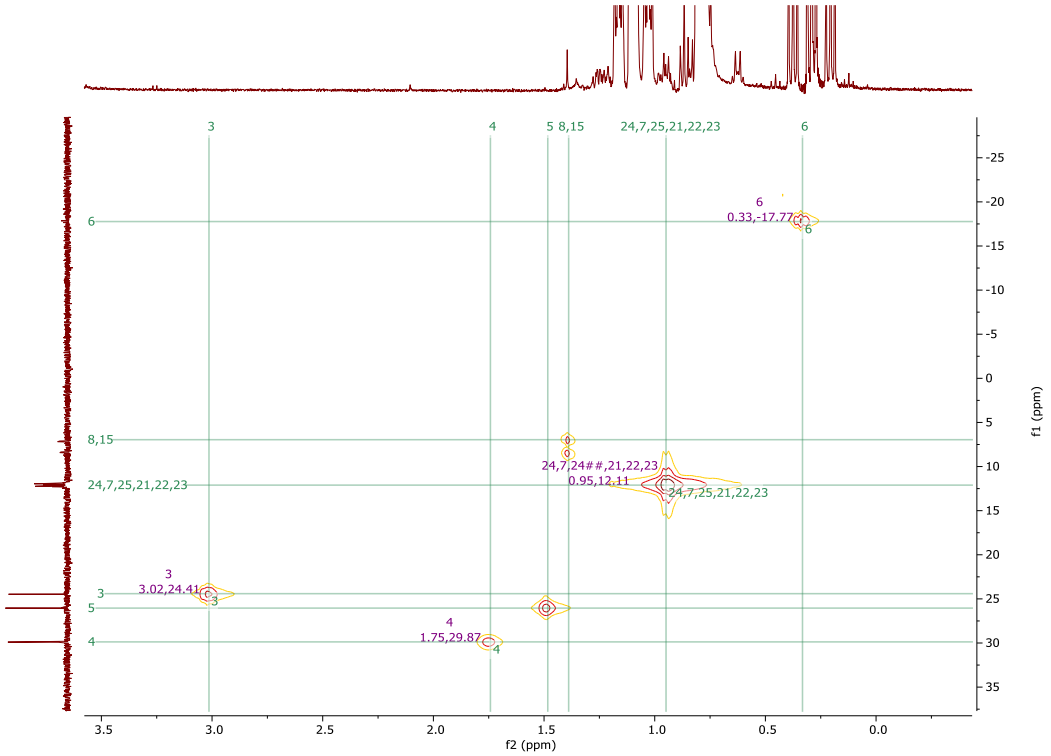

Figure S25. ^{1}H-^{13}C gHSQC spectrum of **Pt(IV)$_{N2}$** (C_6D_6, 400 MHz, 25 °C).

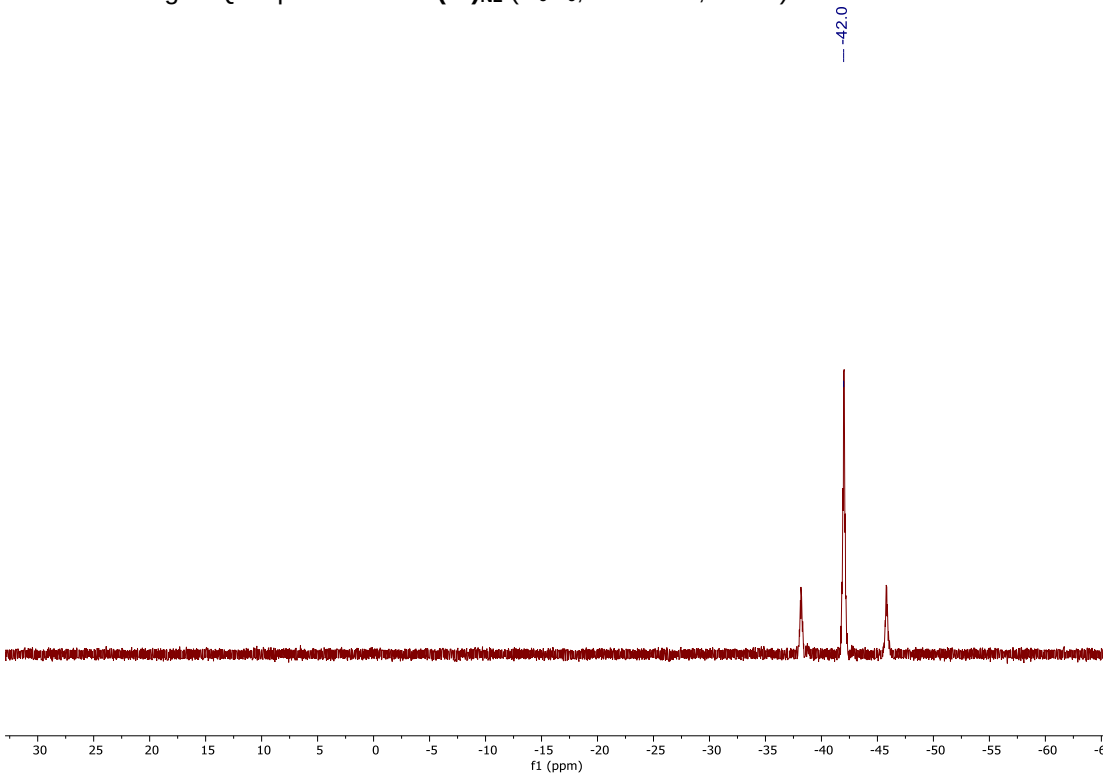

Figure S26. $^{31}P\{^{1}H\}$ NMR spectrum of **Pt(IV)$_{N2}$** (C_6D_6, 162 MHz, 25 °C).

1.10 X-Ray Crystallography of **Pt(IV)$_{N2}$**

X-Ray Intensity data were collected at 100 K on a Bruker Dual micro source D8 Venture diffractometer and PHOTON III detector running APEX3 software package of programs and using Mo Kα radiation (λ = 0.71073 Å). The data frames were integrated and multi-scan scaling was applied in APEX3. Intrinsic phasing structure solution provided all of the non-H atoms.

The structure was refined using full-matrix least-squares refinement.[1] The non-H atoms were refined with anisotropic displacement parameters and all of the H atoms were calculated in idealized positions and refined riding on their parent atoms. In the final cycle of refinement, 7562 reflections (of which 6772 are observed with $I > 2\sigma(I)$) were used to refine 211 parameters and the resulting R_1, wR_2 and S (goodness of fit) were 2.94%, 6.57% and 1.170, respectively. The refinement was carried out by minimizing the wR_2 function using F^2 rather than F values. R_1 is calculated to provide a reference to the conventional R value but its function is not minimized.

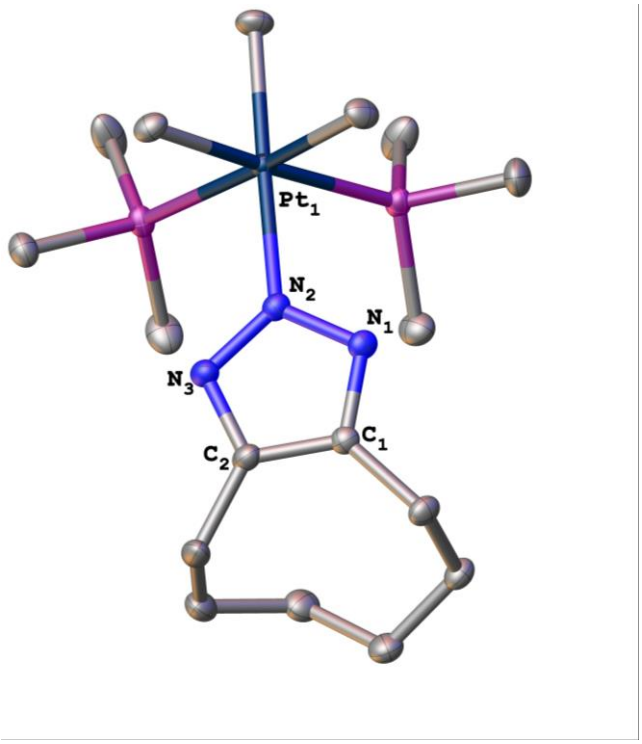

Figure S27. Molecular structure of **Pt(IV)$_{N2}$** (All hydrogen atoms removed for clarity).

Table S5. Crystal data and structure refinement for **Pt(IV)$_{N2}$**.

CCDC Number	**2069850**
Empirical formula	C17 H39 N3 P2 Pt
Formula weight	542.54
Temperature	100(2) K
Wavelength	0.71073 Å
Crystal system	Monoclinic
Space group	P 21/c
Unit cell dimensions	*a* = 7.5376(9) Å, *α*=90°. *b* = 13.5921(17)Å, *β*=98.856(4)°. *c* = 21.634(3) Å, *γ*=90°.
Volume	2190.0(5) Å^3
Z	4
Density (calculated)	1.646 Mg/m^3
Absorption coefficient	6.557 mm^{-1}
F(000)	1080
Crystal size	0.123 x 0.123 x 0.035 mm^3
Theta range for data collection	1.905 to 32.844°.
Index ranges	-11≤h≤11, -20≤k≤20, -32≤l≤32
Reflections collected	58423
Independent reflections	7562 [R(int) = 0.0584]
Completeness to theta = 25.242°	99.5 %
Absorption correction	multi-scan
Refinement method	Full-matrix least-squares on F^2
Data / restraints / parameters	7562 / 0 / 211
Goodness-of-fit on F^2	1.170
Final R indices [I>2sigma(I)]	R_1 = 0.0294, wR_2 = 0.0657 [6772]
R indices (all data)	R_1 = 0.0342, wR_2 = 0.0679
Extinction coefficient	n/a
Largest diff. peak and hole	2.869 and -3.098 e.Å^{-3}

2. Supplementary Computational Data

2.1 Computational Details

Geometries were fully optimized using the Gaussian 09 software package.[9] All relevant minima and transition states were fully optimized in the gas phase at the B3LYP[10,11] level of theory employing correlation-consistent polarized valence double-ζ Dunning (DZ) basis sets with cc-pVDZ quality[12,13] from the EMSL basis set exchange library, using a small core pseudopotential on all metals.[14] All calculations were performed using standard Gaussian 09 SCF convergence criteria with the density fitting approximation (Resolution of Identity, RI)[15–18]. The nature of each stationary point was checked with an analytical second-derivative calculation (no imaginary frequency for minima, exactly one imaginary frequency for transition states, corresponding to the reaction coordinate). Transition states were located using a relaxed potential energy scan to arrive at a suitable transition-state guess, followed by optimization using the Gaussian09 Berny algorithm (opt=ts). The accuracy of the TS was confirmed with an intrinsic reaction coordinate (IRC) scan.[19] Final single-point energies were calculated by employing triple-ζ Dunning (TZ) basis sets (cc-pVTZ quality)[12] while retaining the B3LYP functional. Solvent effects (benzene, ε = 2.27; tetrahydrofuran, ε =7.58; DMSO, ε =46.7 chloroform, ε = 4.81) with the polarizable continuum model approach (PCM) were included in the single point calculations.[20] Grimme dispersion corrections with zero or Becke-Johnson damping (keyword -zero or -bj) were added at this stage using the standalone dftd3 program.[21,22] Enthalpies and Gibbs free energies were then obtained from TZ single-point energies and thermal corrections from the B3LYP/cc-pVDZ-(PP) vibrational analyses (at 298 K and 1 atm); entropy corrections were scaled by a factor of 0.67 to account for decreased entropy in the condensed phase.[23–25] The accuracy of the computational approach was tested by comparing the B3LYP(PCM) results to those obtained using B3LYP with the Solvation Model based on Density (SMD).[26] Further benchmark comparisons used the SMD solvent model for comparison with functionals CAM-B3LYP,[27] MN15 (Gaussian16),[28,29] and ωB97xD.[30] Ultimately, interaction energies and free energy barriers for SPAAC

iClick reactivity exhibited minimal variation and illustrated the same trends. To test the validity of the gas-phase optimization/solvent correction at Single Point Energy stage, the **Au-N_3** system was also fully optimized in solution (THF and $CHCl_3$) indicating also only minimal changes.

Maps of steric bulk were generated using the SambVca 2.0 program providing a calculated. $\Delta\%V_{Bur}$.[31] In all cases, the scanning sphere was centered on N1 , metal and N1 were chosen as z-axis definition, and N2 was chosen as the xz plane definition. Azide nitrogen were deleted, radii scaled to 1.17, sphere radius was set to 5, and mesh spacing set to .1. The distance from center of sphere to coordination sphere was set to 0 and hydrogen atoms were included in the calculation.

2.2 Comparison between X-Ray and Calculated Structures

Table S6. Comparison between the M-N_3 precursor X-Ray structure (Exp) and calculated structures (DFT) optimized at B3LYP/cc-pVDZ level of theory.

Compound	W-N_3 (Exp)	W-N_3 (DFT)	%Error	Au-N_3 (Exp)	Au-N_3 (DFT)	%Error	RuN_3 (Exp)	RuN_3 (DFT)	%Error
M-N1 (Å)	2.18	2.12	3	2.10	2.03	3	2.21	2.13	4
Averaged N1-N2 and N2-N3 (Å)	1.18	1.19	0	1.15	1.18	-3	1.15	1.19	-3
∠M-N1-N2 (°)	125.0	128.5	-3	120.4	123.4	-2	123.6	121.9	1
Compound	**Pt(II)-N_3 (Exp)**	**Pt(II)-N_3 (DFT)**	**%Error**	**Pt(IV)-N_3 (Exp)**	**Pt(IV)-N_3 (DFT)**	**%Error**	**$(PtN_3)_4$ (Exp)**	**$(PtN_3)_4$ (DFT)**	**%Error**
M-N1 (Å)	2.08	2.16	-4	2.17	2.20	-1	2.35	2.32	0
Averaged N1-N2 and N2-N3 (Å)	1.19	1.19	1	1.18	1.19	-1	1.29	1.19	-1
∠M-N1-N2 (°)	127.5	122.9	4	120.7	122.9	-2	122.2	127.3	0

Table S7. Comparison between M-triazolate X-Ray structure (Exp) and calculated structures (DFT) optimized at B3LYP/cc-pVDZ level of theory.

Compound	Au_{N1} (Exp)	Au_{N1} (DFT)	%Error	W_{N2} (Exp)	W_{N2} (DFT)	Error	Re_{N2} (Exp)	Re_{N2} (DFT)	Error
M-N1/N2* (Å)	2.06	2.04	1	2.16	2.16	0	2.15	2.17	-1
Averaged N1-N2 and N2-N3 (Å)	1.28	1.34	-4	1.35	1.34	1	1.34	1.34	0
C-C (triazolate) (Å)	1.37	1.39	-1	1.41	1.42	-1	1.39	1.41	-1
∠M-N1-N2 (°)	119.7	117.1	2	122.2	124.5	-2	122.9	123.9	-1
∠N1-N2-N3 (°)	113.6	108.7	4	111.9	112.3	0	112.5	112.7	0

*M-N1/N2 represents metal bonding to either N1 or N2 of the triazolate.

2.3 FMO Interaction energies

Table S8. B3LYP FMO interaction energies (Δε in eV) between M-N_3 and Cyclooctyne-obtained from distorted TS geometries of each reactant fragment.

	HOMO (eV)		**LUMO (eV)**	
Cyclooctyne	-6.868		-0.578	
	Δε ($HOMO_{CO}$-$LUMO_{az}$)-eV	**Orbital**	**Δε ($HOMO_{az}$-$HOMO_{CO}$)-eV**	**Orbital**
Au-N_3	**-5.238**	LUMO	**-5.822**	HOMO(-1)
AuP(CH_3)$_3$$N_3$	**-5.291**	LUMO	**-5.798**	HOMO(-1)
W-N_3	**-5.443**	LUMO(+1)	**-4.528**	HOMO
Re-N_3	**-5.019**	LUMO(+3)	**-4.521**	HOMO(-1)
Pt(IV)-N_3	**-5.727**	LUMO	**-5.283**	HOMO(-1)
Ru-N_3	**-5.626**	LUMO	**-4.528**	HOMO(-1)
RuP(CH_3)$_3$$N_3$	**-6.12**	LUMO	**-4.444**	HOMO(-1)
Pt(II)-N_3	**-5.853**	LUMO	**-4.976**	HOMO(-1)
PtP(CH_3)$_3$$N_3$	**-5.98**	LUMO	**-5.054**	HOMO(-1)
(PtN_3)$_4$	**-3.996**	LUMO	**-6.1905**	HOMO

*Both normal ($HOMO_{az}$-$LUMO_{CO}$) and inverse electron demand ($HOMO_{CO}$-$LUMO_{az}$) are listed and neither have a significant trend to explain the reactivity difference in the azides.

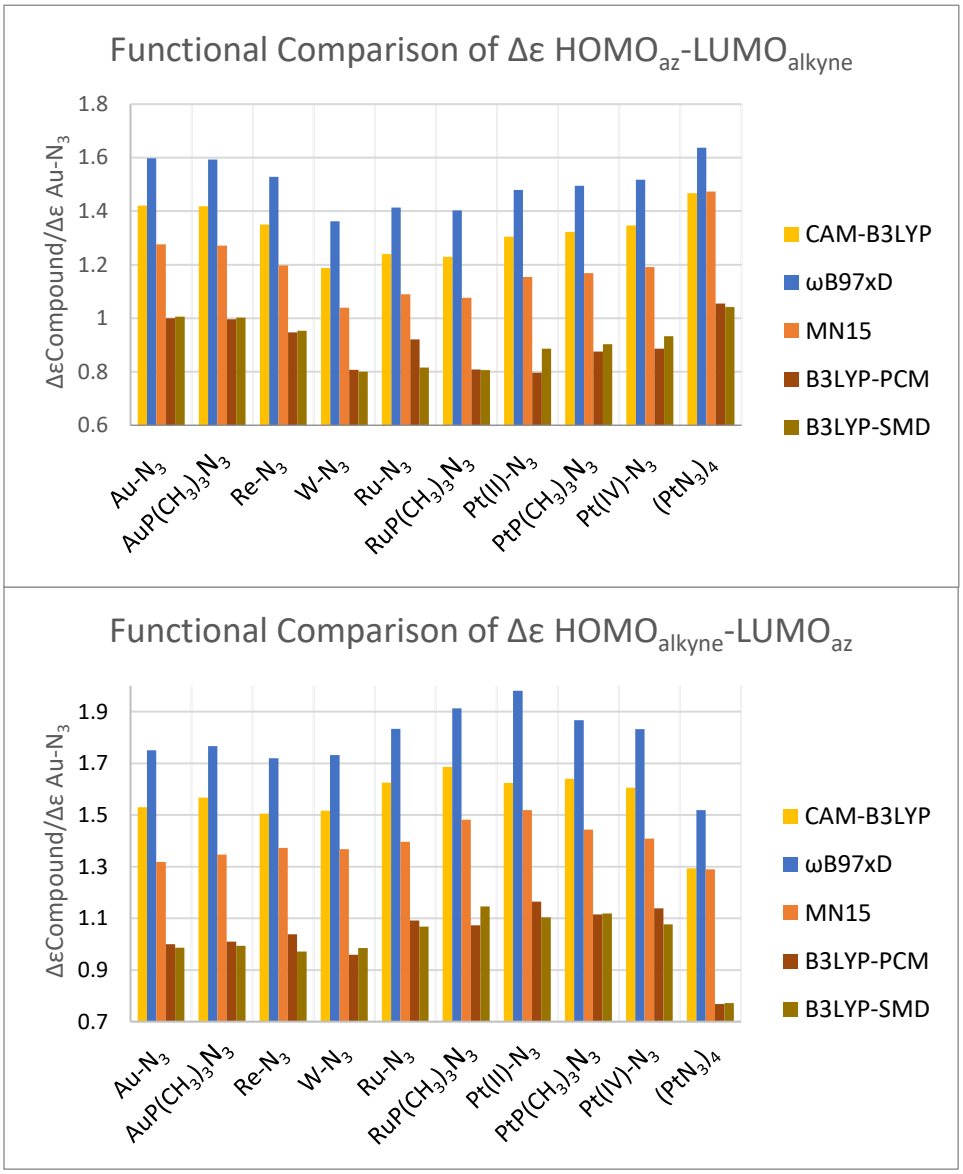

Figure S28. Functional Comparison of FMO Interaction energies. Ratios set to reference of **Au-N$_3$**'s B3LYP interaction energies show that although the magnitude of the energies change, the general trend remains very close between all four functionals.

2.4 SambVCA % Buried Volume (%V_{bur}) of **M-N_3**

Table S9. SambVCA Steric Analysis- % Buried Volume (%V_{bur}) of M-N_3 where cyclooctyne approaches.

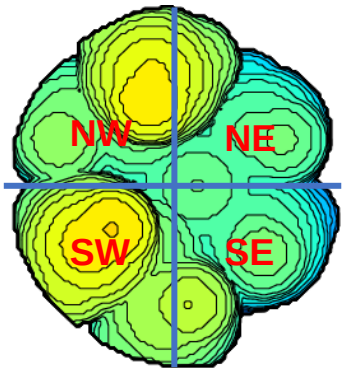

%V_{bur}	Total	SW	NW	NE	SE
Ru-N_3	63.1	74.7	73.0	57.9	46.8
Pt(II)-N_3	52.6	67.6	42.1	59.3	41.4
$(PtN_3)_4$	68.3	93.5	93.5	42.2	43.8
Au-N_3	14.6	15.7	16.7	13.2	12.7
AuP$(CH_3)_3N_3$	11.1	11.8	11.9	10.3	10.3
W-N_3	42.7	53.5	53.2	31.9	32.2
Re-N_3	38.2	29.8	30.0	46.7	46.4
RuP$(CH_3)_3N_3$	50.7	56.7	50.9	42.4	52.9
Pt(IV)-N_3	43.9	57.0	54.4	31.4	32.9
PtP$(CH_3)_3N_3$	35.2	55.6	16.2	49.7	19.3
Pt$(CH_3)_3N_3$	18.3	22.9	22.4	13.6	14.5

*The red highlighted rows represent azides with high calculated SPAAC iClick barriers and the green rows represent azides with low calculated barriers.

2.5 SambVCA Steric Map of **$(PtN_3)_4$** and $Pt(CH_3)_3N_3$

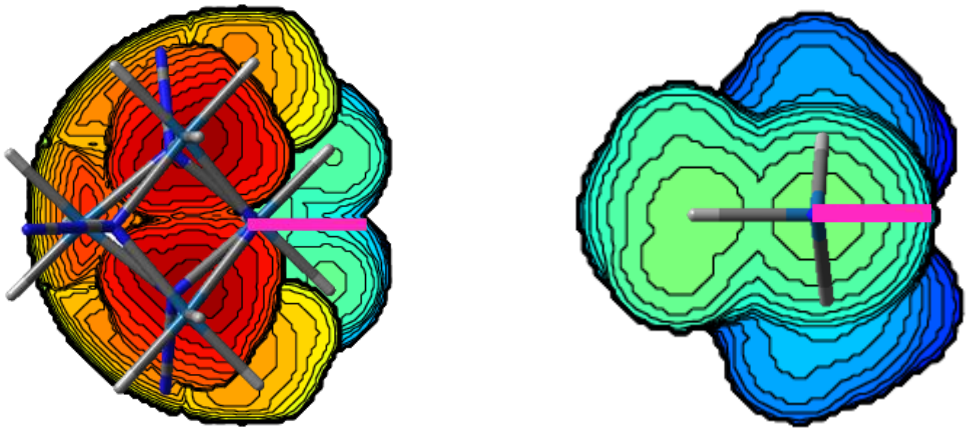

Figure S29. The steric map of the tetrameric (**$(PtN_3)_4$**, left) and monomeric ($Pt(CH_3)_3N_3$, right) (azide centered to right and colored pink for emphasis; blue to red represents increasing steric bulk) suggests that the cluster is too sterically hindered to react with cyclooctyne (%V_{bur}=68.3; ΔG=41.0 kcal/mol) and requires theoretical dissociation to react (%V_{bur}=18.3; ΔG=21.4 kcal/mol).

2.6 SambVCA Steric Map of **Pt(IV)-N_3**'s Reacting Azide

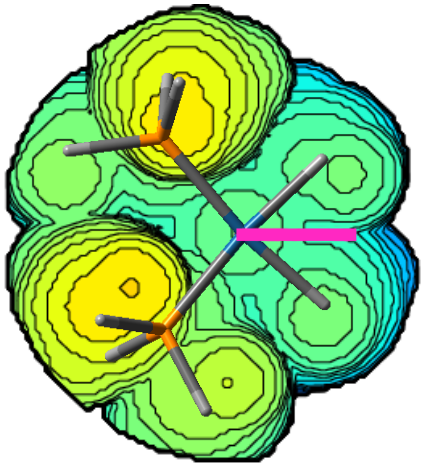

Figure S30. The steric map of **Pt(IV)-N_3** (azide centered to right and colored pink for emphasis; blue to red represents increasing steric bulk) illustrates ample space for the alkyne to approach for cycloaddition. While not as free as the linear **Au-N_3**, the steric profile of **Pt(IV)-N_3** resembles that of the other octahedral complexes **Re-N_3** and **W-N_3**. The %V_{bur} of 43.9 is comparable to **Re-N_3** and **W-N_3**, supporting this assessment.

2.7 Comparison of Potential Energy Surfaces of **Ru-N_3** and $RuP(CH_3)_3N_3$

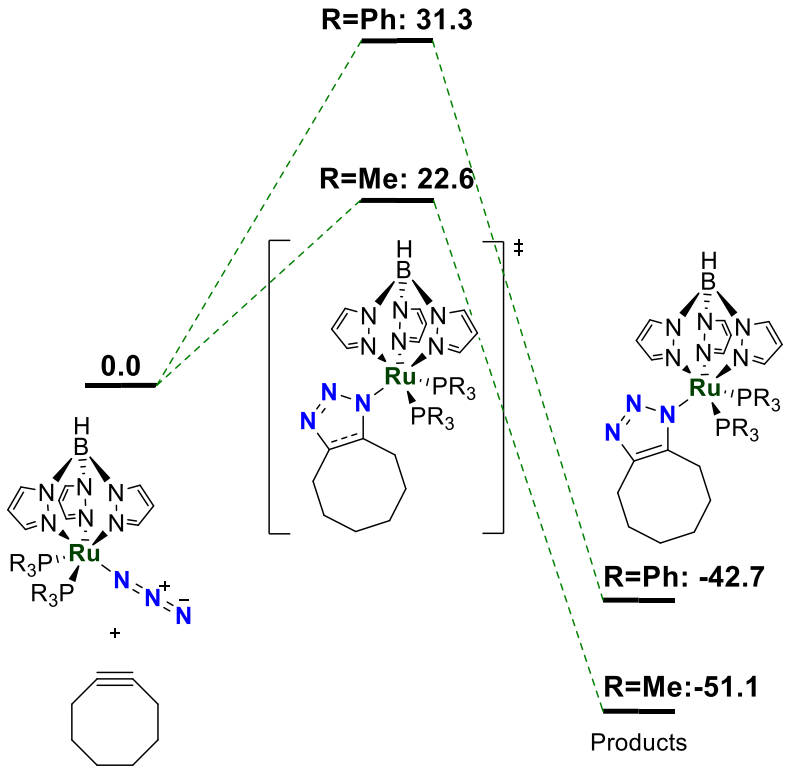

2.7 Energy Tables of SPAAC iClick Reactivity

Table S10. Final Energies, Enthalpy and Entropy Corrections, Gibbs Free Energies from B3LYP functional with Becke-Johnson Damping Dispersion Correction-D3. In Hartree. See Computational Details for Methods.

Metal (Solvent)	Structure	E(B3LYP/cc-pVDZ)	E(B3LYP(PCM)/cc-pVTZ)	ZPE	D3	$H_{correction}$	$S_{correction}$	G
	CycloOctyne (Benzene)	-312.0112817	-312.1140186	0.178609	-0.0327634	0.187449	0.040713	-311.9866107
	CycloOctyne (DMSO)	-312.0112817	-312.1157522	0.178609	-0.0327634	0.187449	0.040713	-311.9883443
	CycloOctyne (THF)	-312.0112817	-312.1151749	0.178609	-0.0327634	0.187449	0.040713	-311.9877670
Au (THF)	**Au-N_3**	-1336.400865	-1336.680478	0.287366	-0.1051097	0.3099670	0.0797820	-1336.529075
	Au-N_3cycloOctyneClickTS	-1648.390182	-1648.764762	0.466427	-0.1476348	0.4978340	0.1015660	-1648.482612
	Au_{N1}	-1648.524278	-1648.897576	0.472385	-0.1509492	0.5021336	0.0957479	-1648.610542
	AuN1toN2isomerizationTS	-1648.500527	-1648.870785	0.471638	-0.1498146	0.5021336	0.0949481	-1648.582081
	Au_{N2}	-1648.531755	-1648.900461	0.472742	-0.1484851	0.5022628	0.0978821	-1648.612264
	$AuP(CH_3)_3N_3$	-761.1649753	-761.3006787	0.126565	-0.0327180	0.139606	0.054867	-761.2305516
	$AuP(CH_3)_3N_3$cycloOctyneClickTS	-1073.154266	-1073.384934	0.305784	-0.0749792	0.327519	0.074896	-1073.182575
	$AuP(CH_3)_3N_3$cycloOctyneProduct	-1073.288016	-1073.518059	0.311716	-0.0780682	0.331866	0.070552	-1073.311531
Re (DMSO)	**Re-N_3**	-1078.457350	-1078.766416	0.199196	-0.0867308	0.220220	0.071925	-1078.681116
	Re-N_3cycloOctyneClickTS	-1390.446088	-1390.850878	0.378198	-0.1307250	0.408069	0.094196	-1390.636645
	Re_{N1}	-1390.584551	-1390.981024	0.384948	-0.1345058	0.412937	0.086961	-1390.760857
	ReN1toN2isomerizationTS	-1390.551564	-1390.947682	0.383644	-0.1360849	0.411254	0.086821	-1390.730683
	Re_{N2}	-1390.590465	-1390.986143	0.384732	-0.1308227	0.412875	0.088299	-1390.763251
Ru (C_6H_6)	**Ru-N_3**	-3034.102610	-3034.767203	0.765927	-0.3423641	0.817797	0.138321	-3034.384445
	Ru-N_3cycloOctyneClickTS	-3346.080393	-3346.829010	0.945198	-0.3950841	1.005568	0.157136	-3346.323807
	Ru-N_3cycloOctyneProduct	-3346.193681	-3346.947212	0.951687	-0.4043638	1.010572	0.152519	-3346.443191
	$RuP(CH_3)_3N_3$	-1883.655948	-1884.035381	0.443302	-0.1647307	0.476204	0.093735	-1883.786710
	$RuP(CH_3)_3N_3$cycloOctyneClickTS	-2195.639437	-2196.112977	0.622629	-0.2150462	0.664117	0.112933	-2195.739571
	$RuP(CH_3)_3N_3$cycloOctyneProduct	-2195.764332	-2196.233333	0.629223	-0.2216957	0.669111	0.108089	-2195.858338

Table S10 Cont'd. Final Energies, Enthalpy and Entropy Corrections, Gibbs Free Energies from B3LYP functional with Becke-Johnson Damping Dispersion Correction-D3. In Hartree. See Computational Details for Methods.

Metal (Solvent)	Structure	E(B3LYP/cc-pVDZ)	E(B3LYP(PCM)/cc-pVTZ)	ZPE	D3	$H_{correction}$	$S_{correction}$	G
Pt(II) (C_6H_6)	**Pt(II)-N_3**	-1717.690972	-1718.054753	0.618443	-0.0811448	0.657461	0.107616	-1717.550540
	Pt(II)-N_3cycloOctyneClickTS	-2029.665348	-2030.122633	0.798756	-0.1292793	0.845824	0.124214	-2029.489312
	Pt(II)-N_3cycloOctyneProduct	-2029.802561	-2030.254797	0.805156	-0.1330729	0.850693	0.119924	-2029.617526
	Pt(II)P(CH_3)$_3N_3$	-1245.962269	-1246.175479	0.277118	-0.1839324	0.300167	0.074648	-1246.109259
	Pt(II)P(CH_3)$_3N_3$cycloOctyneClickTS	-1557.949114	-1558.256107	0.456503	-0.2355753	0.488118	0.094588	-1558.066938
	Pt(II)P(CH_3)$_3N_3$cycloOctyneProduct	-1558.084680	-1558.387232	0.462364	-0.2404881	0.492493	0.090608	-1558.195935
W (DMSO)	**W-N_3**	-1071.236245	-1071.549879	0.260776	-0.1024593	0.283259	0.073804	-1071.418528
	W-N_3cycloOctyneClickTS	-1382.641196	-1383.631922	0.440151	-0.1507867	0.471281	0.093700	-1383.374207
	W_{N1}	-1383.357342	-1383.757985	0.446884	-0.1560650	0.476217	0.088260	-1383.496967
	WN1toN2isomerizationTS	-1382.753024	-1383.735666	0.445900	-0.1526201	0.474839	0.088250	-1383.472574
	W_{N2}	-1382.781085	-1383.767010	0.446700	-0.1511211	0.476169	0.089452	-1383.501895
Pt(IV) (C_6H_6)	**Pt(IV)-N_3**	-1325.737086	-1325.981298	0.352443	-0.1086413	0.379196	0.080820	-1325.764893
	Pt(IV)-N_3cycloOctyneClickTS	-1637.722330	-1638.060033	0.531872	-0.1569944	0.567109	0.100079	-1637.716971
	$Pt(IV)_{N1}$	-1637.861677	-1638.192187	0.538496	-0.1619954	0.572073	0.095106	-1637.845831
	Pt(IV)N1toN2isomerizationTS	-1637.831218	-1638.159893	0.536274	-0.1592626	0.569904	0.096576	-1637.813958
	$Pt(IV)_{N2}$	-1637.870653	-1638.198904	0.537858	-0.1574014	0.571815	0.097123	-1637.849563
$(PtN_3)_4$ (C_6H_6)	**$(PtN_3)_4$**	-1613.945159	-1614.330660	0.497548	-0.16679008	0.544877	0.126006	-1614.037000
	$(PtN_3)_4$cycloOctyneClickTS	-1925.900653	-1926.381940	0.678575	-0.19682025	0.733991	0.143592	-1925.94098
	$(PtN_3)_4$cycloOctyneProduct	-1926.049509	-1926.524200	0.686608	-0.20574788	0.739804	0.137470	-1926.08225
	Pt(CH_3)$_3N_3$	-403.4286385	-403.5392210	0.121835	-0.02778111	0.134056	0.082470	0.051586
	Pt(CH_3)$_3N_3$cycloOctyneClickTS	-715.4190124	-715.6239696	0.301254	-0.07171153	0.322014	0.250004	0.072010
	Pt(CH_3)$_3N_3$cycloOctyneProduct	-715.5486168	-715.7518136	0.307045	-0.07455223	0.326108	0.259540	0.066568

Table S11. Final Energies, Enthalpy and Entropy Corrections, Gibbs Free Energies from B3LYP functional with Zero Damping Dispersion Correction-D0. In Hartree. See Computational Details for Methods.

Metal (Solvent)	Structure	E(B3LYP/cc-pVDZ)	E(B3LYP(PCM)/cc-pVTZ)	ZPE	D0	$H_{correction}$	$S_{correction}$	G
	CycloOctyne (Benzene)	-312.0112817	-312.1140186	0.178609	-0.0155483	0.187449	0.040713	-311.9693956
	CycloOctyne (DMSO)	-312.0112817	-312.1157522	0.178609	-0.0155483	0.187449	0.040713	-311.9711292
	CycloOctyne (THF)	-312.0112817	-312.1151749	0.178609	-0.0155483	0.187449	0.040713	-311.9705519
Au (THF)	**Au-N_3**	-1336.400865	-1336.680478	0.287366	-0.0447659	0.309967	0.079782	-1336.468731
	Au-N_3cycloOctyneClickTS	-1648.390182	-1648.764762	0.466427	-0.0678001	0.497834	0.101566	-1648.402777
	Au_{N1}	-1648.524278	-1648.897576	0.472385	-0.0704289	0.502134	0.095748	-1648.530022
	AuN1toN2isomerizationTS	-1648.500527	-1648.870785	0.471638	-0.0691839	0.502134	0.094948	-1648.501450
	Au_{N2}	-1648.531755	-1648.900461	0.472742	-0.0682811	0.502263	0.097882	-1648.532060
	$AuP(CH_3)_3N_3$	-761.1649753	-761.3006787	0.126565	-0.0135970	0.139606	0.054867	-761.2114305
	$AuP(CH_3)_3N_3$cycloOctyneClickTS	-1073.154266	-1073.384934	0.305784	-0.0363511	0.327519	0.074896	-1073.143947
	$AuP(CH_3)_3N_3$cycloOctyneProduct	-1073.288016	-1073.518059	0.311716	-0.0387612	0.331866	0.070552	-1073.272224
Re (DMSO)	**Re-N_3**	-1078.457350	-1078.766416	0.199196	-0.0408405	0.220220	0.071925	-1078.635226
	Re-N_3cycloOctyneClickTS	-1390.446088	-1390.850878	0.378198	-0.0656304	0.408069	0.094196	-1390.571550
	Re_{N1}	-1390.584551	-1390.981024	0.384948	-0.0686342	0.412937	0.086961	-1390.694985
	ReN1toN2isomerizationTS	-1390.551564	-1390.947682	0.383644	-0.0697456	0.411254	0.086821	-1390.664343
	Re_{N2}	-1390.590465	-1390.986143	0.384732	-0.0645756	0.412875	0.088299	-1390.697004
Ru (C_6H_6)	**Ru-N_3**	-3034.102610	-3034.767203	0.765927	-0.1809022	0.817797	0.138321	-3034.222984
	Ru-N_3cycloOctyneClickTS	-3346.080393	-3346.829010	0.945198	-0.2138496	1.005568	0.157136	-3346.142573
	Ru-N_3cycloOctyneProduct	-3346.193681	-3346.947212	0.951687	-0.2216199	1.010572	0.152519	-3346.260447
	$RuP(CH_3)_3N_3$	-1883.655948	-1884.035381	0.443302	-0.0889423	0.476204	0.093735	-1883.710921
	$RuP(CH_3)_3N_3$cycloOctyneClickTS	-2195.639437	-2196.112977	0.622629	-0.1197783	0.664117	0.112933	-2195.644303
	$RuP(CH_3)_3N_3$cycloOctyneProduct	-2195.764332	-2196.233333	0.629223	-0.1250369	0.669111	0.108089	-2195.761679

Table S11 Cont'd. Final Energies, Enthalpy and Entropy Corrections, Gibbs Free Energies from B3LYP functional with Zero Damping Dispersion Correction-D0. In Hartree. See Computational Details for Methods.

Metal (Solvent)	Structure	E(B3LYP/cc-pVDZ)	E(B3LYP(PCM)/cc-pVTZ)	ZPE	D0	$H_{correction}$	$S_{correction}$	G
Pt(II) (C_6H_6)	**Pt(II)-N_3**	-1717.690972	-1718.054753	0.618443	-0.1170845	0.657461	0.107616	-1717.586480
	Pt(II)-N_3cycloOctyneClickTS	-2029.665348	-2030.122633	0.798756	-0.1492831	0.845824	0.124214	-2029.509316
	Pt(II)-N_3cycloOctyneProduct	-2029.802561	-2030.254797	0.805156	-0.1539903	0.850693	0.119924	-2029.638444
	Pt(II)P(CH_3)$_3$	-1245.962269	-1246.175479	0.277118	-0.0428644	0.300167	0.074648	-1245.968191
	Pt(II)P(CH_3)$_3$$N_3$cycloOctyneClickTS	-1557.949114	-1558.256107	0.456503	-0.0716184	0.488118	0.094588	-1557.902981
	Pt(II)P(CH_3)$_3$$N_3$cycloOctyneProduct	-1558.084680	-1558.387232	0.462364	-0.0753415	0.492493	0.090608	-1558.030788
W (DMSO)	**W-N_3**	-1071.236245	-1071.549879	0.260776	-0.0510594	0.283259	0.073804	-1071.367128
	W-N_3cycloOctyneClickTS	-1382.641196	-1383.631922	0.440151	-0.0799072	0.471281	0.093700	-1383.303327
	W_{N1}	-1383.357342	-1383.757985	0.446884	-0.0841009	0.476217	0.088260	-1383.425003
	WN1toN2isomerizationTS	-1382.753024	-1383.735666	0.445900	-0.0804442	0.474839	0.088250	-1383.400398
	W_{N2}	-1382.781085	-1383.767010	0.446700	-0.0788480	0.476169	0.089452	-1383.429622
Pt(IV) (C_6H_6)	**Pt(IV)-N_3**	-1325.737086	-1325.981298	0.352443	-0.0617869	0.379196	0.080820	-1325.718038
	Pt(IV)-N_3cycloOctyneClickTS	-1637.722330	-1638.060033	0.531872	-0.0904516	0.567109	0.100079	-1637.650428
	Pt(IV)$_{N1}$	-1637.861677	-1638.192187	0.538496	-0.0952243	0.572073	0.095106	-1637.779059
	Pt(IV)N1toN2isomerizationTS	-1637.831218	-1638.159893	0.536274	-0.0918625	0.569904	0.096576	-1637.746558
	Pt(IV)$_{N2}$	-1637.870653	-1638.198904	0.537858	-0.0904980	0.571815	0.097123	-1637.782659
(PtN_3)$_4$ (C_6H_6)	**(PtN_3)$_4$**	-1613.945159	-1614.33066	0.497548	-0.16679008	0.544877	0.126006	-1614.037000
	(PtN_3)$_4$cycloOctyneClickTS	-1925.900653	-1926.38194	0.678575	-0.19682025	0.733991	0.143592	-1925.94098
	(PtN_3)$_4$cycloOctyneProduct	-1926.049509	-1926.52420	0.686608	-0.20574788	0.739804	0.137470	-1926.082248
	Pt(CH_3)$_3$$N_3$	-403.4286385	-403.539221	0.121835	-0.01254500	0.134056	0.051586	-403.4522727
	Pt(CH_3)$_3$$N_3$cycloOctyneClickTS	-715.4190124	-715.6239696	0.301254	-0.03732541	0.322014	0.072010	-715.3875277
	Pt(CH_3)$_3$$N_3$cycloOctyneProduct	-715.5486168	-715.7518136	0.307045	-0.03985185	0.326108	0.066568	-715.5101580

Table S12. Final Energies, Enthalpy and Entropy Corrections, Gibbs Free Energies from B3LYP functional with Zero Damping Dispersion Correction-D0 and SMD solvent model. In Hartree. See Computational Details for Methods.

Metal (Solvent)	Structure	E(B3LYP/cc-pVDZ)	E(B3LYP(SMD)/cc-pVTZ)	ZPE	D0	$H_{correction}$	$S_{correction}$	G
	CycloOctyne (Benzene)	-312.0112817	-312.1229881	0.178609	-0.0155483	0.187449	0.040713	-311.9783651
	CycloOctyne (DMSO)	-312.0112817	-312.1203944	0.178609	-0.0155483	0.187449	0.040713	-311.9757714
	CycloOctyne (THF)	-312.0112817	-312.1226055	0.178609	-0.0155483	0.187449	0.040713	-311.9779825
Au (THF)	**Au-N_3**	-1336.400865	-1336.690975	0.287366	-0.0447659	0.309967	0.079782	-1336.479228
	Au-N_3cycloOctyneClickTS	-1648.390182	-1648.783155	0.466427	-0.0678001	0.497834	0.101566	-1648.421170
	Au_{N1}	-1648.524278	-1648.917716	0.472385	-0.0704289	0.502134	0.095748	-1648.550162
	AuN1toN2isomerizationTS	-1648.500527	-1648.890789	0.471638	-0.0691839	0.502134	0.094948	-1648.521454
	Au_{N2}	-1648.531755	-1648.920382	0.472742	-0.0682811	0.502263	0.097882	-1648.551982
	$AuP(CH_3)_3N_3$	-761.1649753	-761.2996061	0.126565	-0.0135970	0.139606	0.054867	-761.2103579
	$AuP(CH_3)_3N_3$cycloOctyneClickTS	-1073.154266	-1073.391857	0.305784	-0.0363511	0.327519	0.074896	-1073.150870
	$AuP(CH_3)_3N_3$cycloOctyneProduct	-1073.288016	-1073.526520	0.311716	-0.0387612	0.331866	0.070552	-1073.280685
Re (DMSO)	**Re-N_3**	-1078.457350	-1078.770755	0.199196	-0.0408405	0.220220	0.071925	-1078.639566
	Re-N_3cycloOctyneClickTS	-1390.446088	-1390.861903	0.378198	-0.0656304	0.408069	0.094196	-1390.582575
	Re_{N1}	-1390.584551	-1390.992991	0.384948	-0.0686342	0.412937	0.086961	-1390.706952
	ReN1toN2isomerizationTS	-1390.551564	-1390.959479	0.383644	-0.0697456	0.411254	0.086821	-1390.676141
	Re_{N2}	-1390.590465	-1390.997702	0.384732	-0.0645756	0.412875	0.088299	-1390.708563
Ru (C_6H_6)	**Ru-N_3**	-3034.102610	-3034.801162	0.765927	-0.1809022	0.817797	0.138321	-3034.256942
	Ru-N_3cycloOctyneClickTS	-3346.080393	-3346.870766	0.945198	-0.2138496	1.005568	0.157136	-3346.184329
	Ru-N_3cycloOctyneProduct	-3346.193681	-3346.988769	0.951687	-0.2216199	1.010572	0.152519	-3346.302004
	$RuP(CH_3)_3N_3$	-1883.655948	-1884.045108	0.443302	-0.0889423	0.476204	0.093735	-1883.720648
	$RuP(CH_3)_3N_3$cycloOctyneClickTS	-2195.639437	-2196.13046	0.622629	-0.1197783	0.664117	0.112933	-2195.661787
	$RuP(CH_3)_3N_3$cycloOctyneProduct	-2195.764332	-2196.251424	0.629223	-0.1250369	0.669111	0.108089	-2195.779769

Table S12 Cont'd. Final Energies, Enthalpy and Entropy Corrections, Gibbs Free Energies from B3LYP functional with Zero Damping Dispersion Correction-D0 and SMD solvent model. In Hartree. See Computational Details for Methods.

Metal (Solvent)	Structure	E(B3LYP/cc-pVDZ)	E(B3LYP(SMD)/cc-pVTZ)	ZPE	D0	$H_{correction}$	$S_{correction}$	G
Pt(II) (C_6H_6)	**Pt(II)-N_3**	-1717.690972	-1718.065656	0.618443	-0.1170845	0.657461	0.107616	-1717.597382
	Pt(II)-N_3cycloOctyneClickTS	-2029.665348	-2030.140972	0.798756	-0.1492831	0.845824	0.124214	-2029.527654
	Pt(II)-N_3cycloOctyneProduct	-2029.802561	-2030.272943	0.805156	-0.1539903	0.850693	0.119924	-2029.656590
	Pt(II)P(CH_3)$_3$	-1245.962269	-1246.175558	0.277118	-0.0428644	0.300167	0.074648	-1245.968270
	Pt(II)P(CH_3)$_3$$N_3$cycloOctyneClickTS	-1557.949114	-1558.264622	0.456503	-0.0716184	0.488118	0.094588	-1557.911496
	Pt(II)P(CH_3)$_3$$N_3$cycloOctyneProduct	-1558.084680	-1558.396407	0.462364	-0.0753415	0.492493	0.090608	-1558.039962
W (DMSO)	**W-N_3**	-1071.236245	-1071.556186	0.260776	-0.0510594	0.283259	0.073804	-1071.373435
	W-N_3cycloOctyneClickTS	-1382.641196	-1383.644398	0.440151	-0.0799072	0.471281	0.093700	-1383.315803
	W_{N1}	-1383.357342	-1383.771627	0.446884	-0.0841009	0.476217	0.088260	-1383.438645
	WN1toN2isomerizationTS	-1382.753024	-1383.749388	0.445900	-0.0804442	0.474839	0.088250	-1383.414120
	W_{N2}	-1382.781085	-1383.780834	0.446700	-0.0788480	0.476169	0.089452	-1383.443445
Pt(IV) (C_6H_6)	**Pt(IV)-N_3**	-1325.737086	-1325.983030	0.352443	-0.0617869	0.379196	0.080820	-1325.719770
	Pt(IV)-N_3cycloOctyneClickTS	-1637.722330	-1638.070634	0.531872	-0.0904516	0.567109	0.100079	-1637.661030
	$Pt(IV)_{N1}$	-1637.861677	-1638.203100	0.538496	-0.0952243	0.572073	0.095106	-1637.789973
	Pt(IV)N1toN2isomerizationTS	-1637.831218	-1638.170305	0.536274	-0.0918625	0.569904	0.096576	-1637.756969
	$Pt(IV)_{N2}$	-1637.870653	-1638.210777	0.537858	-0.0904980	0.571815	0.097123	-1637.794532
$(PtN_3)_4$ (C_6H_6)	**$(PtN_3)_4$**	-1613.945159	-1614.326721	0.497548	-0.16679008	0.544877	0.126006	-1614.033058
	$(PtN_3)_4$cycloOctyneClickTS	-1925.900653	-1926.385683	0.678575	-0.19682025	0.733991	0.143592	-1925.944718
	$(PtN_3)_4$cycloOctyneProduct	-1926.049509	-1926.527500	0.686608	-0.20574788	0.739804	0.137470	-1926.085548
	Pt(CH_3)$_3$$N_3$	-403.4286385	-403.5331834	0.121835	-0.01254500	0.134056	0.051586	-403.4462350
	Pt(CH_3)$_3$$N_3$cycloOctyneClickTS	-715.4190124	-715.6274874	0.301254	-0.03732541	0.322014	0.072010	-715.3910455
	Pt(CH_3)$_3$$N_3$cycloOctyneProduct	-715.5486168	-715.7562360	0.307045	-0.03985185	0.326108	0.066568	-715.5145804

Table S13. Final Energies, Enthalpy and Entropy Corrections, Gibbs Free Energies from CAM-B3LYP with Zero Damping Dispersion Correction-D0 and SMD solvent model. In Hartree. See Computational Details for Methods.

Metal (Solvent)	Structure	E(B3LYP/cc-pVDZ)	E(CAM-B3LYP(SMD)/cc-pVTZ)	ZPE	D0	$H_{correction}$	$S_{correction}$	G
	CycloOctyne (Benzene)	-312.0112817	-311.9278447	0.178609	-0.0106438	0.187449	0.040713	-311.7783172
	CycloOctyne (DMSO)	-312.0112817	-311.9253923	0.178609	-0.0106438	0.187449	0.040713	-311.7758648
	CycloOctyne (THF)	-312.0112817	-311.9275593	0.178609	-0.0106438	0.187449	0.040713	-311.7780318
Au (THF)	**Au-N_3**	-1336.400865	-1336.101311	0.287366	-0.0312787	0.309967	0.079782	-1335.876077
	Au-N_3cycloOctyneClickTS	-1648.390182	-1647.999001	0.466427	-0.0473311	0.497834	0.101566	-1647.616547
	Au_{N1}	-1648.524278	-1648.149641	0.472385	-0.0492827	0.502134	0.095748	-1647.760941
	AuN1toN2isomerizationTS	-1648.500527	-1648.121927	0.471638	-0.0483791	0.502134	0.094948	-1647.731787
	Au_{N2}	-1648.531755	-1648.152366	0.472742	-0.0477090	0.502263	0.097882	-1647.763393
	$AuP(CH_3)_3N_3$	-761.1649753	-761.0384849	0.126565	-0.0093130	0.139606	0.054867	-760.9449527
	$AuP(CH_3)_3N_3$cycloOctyneClickTS	-1073.154266	-1072.936252	0.305784	-0.0250934	0.327519	0.074896	-1072.684007
	$AuP(CH_3)_3N_3$cycloOctyneProduct	-1073.288016	-1073.086890	0.311716	-0.0268416	0.331866	0.070552	-1072.829136
Re (DMSO)	**Re-N_3**	-1078.457350	-1078.214697	0.199196	-0.0283039	0.220220	0.071925	-1078.070971
	Re-N_3cycloOctyneClickTS	-1390.446088	-1390.111471	0.378198	-0.0457526	0.408069	0.094196	-1389.812266
	Re_{N1}	-1390.584551	-1390.259725	0.384948	-0.0480141	0.412937	0.086961	-1389.953066
	ReN1toN2isomerizationTS	-1390.551564	-1390.224398	0.383644	-0.0487082	0.411254	0.086821	-1389.920023
	Re_{N2}	-1390.590465	-1390.263751	0.384732	-0.0452963	0.412875	0.088299	-1389.955332
Ru (C_6H_6)	**Ru-N_3**	-3034.102610	-3033.471868	0.765927	-0.1275687	0.817797	0.138321	-3032.874315
	Ru-N_3cycloOctyneClickTS	-3346.080393	-3345.347836	0.945198	-0.1510490	1.005568	0.157136	-3344.598598
	Ru-N_3cycloOctyneProduct	-3346.193681	-3345.483865	0.951687	-0.1566343	1.010572	0.152519	-3344.732115
	$RuP(CH_3)_3N_3$	-1883.655948	-1883.368548	0.443302	-0.0621572	0.476204	0.093735	-1883.017304
	$RuP(CH_3)_3N_3$cycloOctyneClickTS	-2195.639437	-2195.259908	0.622629	-0.0838714	0.664117	0.112933	-2194.755328
	$RuP(CH_3)_3N_3$cycloOctyneProduct	-2195.764332	-2195.398533	0.629223	-0.0877451	0.669111	0.108089	-2194.889587

Table S13 Cont'd. Final Energies, Enthalpy and Entropy Corrections, Gibbs Free Energies from CAM-B3LYP with Zero Damping Dispersion Correction-D0 and SMD solvent model. In Hartree. See Computational Details for Methods.

Metal (Solvent)	Structure	E(B3LYP/cc-pVDZ)	E(CAM-B3LYP/cc-pVTZ)	ZPE	D0	$H_{correction}$	$S_{correction}$	G
Pt(II) (C_6H_6)	**Pt(II)-N_3**	-1717.690972	-1717.39231	0.618443	-0.0821357	0.657461	0.107616	-1716.889088
	Pt(II)-N_3cycloOctyneClickTS	-2029.665348	-2029.274564	0.798756	-0.1051803	0.845824	0.124214	-2028.617143
	Pt(II)-N_3cycloOctyneProduct	-2029.802561	-2029.42349	0.805156	-0.1084467	0.850693	0.119924	-2028.761593
	Pt(II)P(CH_3)$_3$	-1245.962269	-1245.796973	0.277118	-0.0296982	0.300167	0.074648	-1245.576519
	Pt(II)P(CH_3)$_3$$N_3$cycloOctyneClickTS	-1557.949114	-1557.692539	0.456503	-0.0498712	0.488118	0.094588	-1557.317666
	Pt(II)P(CH_3)$_3$$N_3$cycloOctyneProduct	-1558.084680	-1557.840762	0.462364	-0.0524398	0.492493	0.090608	-1557.461417
W (DMSO)	**W-N_3**	-1071.236245	-1070.9726	0.260776	-0.0356631	0.283259	0.073804	-1070.774453
	W-N_3cycloOctyneClickTS	-1382.641196	-1382.86685	0.440151	-0.0558602	0.471281	0.093700	-1382.514209
	W_{N1}	-1383.357342	-1383.011999	0.446884	-0.0590106	0.476217	0.088260	-1382.653927
	WN1toN2isomerizationTS	-1382.753024	-1382.988549	0.445900	-0.0564015	0.474839	0.088250	-1382.629239
	W_{N2}	-1382.781085	-1383.020192	0.446700	-0.0554063	0.476169	0.089452	-1382.659362
Pt(IV) (C_6H_6)	**Pt(IV)-N_3**	-1325.737086	-1325.54841	0.352443	-0.0428604	0.379196	0.080820	-1325.266224
	Pt(IV)-N_3cycloOctyneClickTS	-1637.722330	-1637.442415	0.531872	-0.06306	0.567109	0.100079	-1637.005418
	Pt(IV)$_{N1}$	-1637.861677	-1637.592517	0.538496	-0.0664974	0.572073	0.095106	-1637.150662
	Pt(IV)N1toN2isomerizationTS	-1637.831218	-1637.555619	0.536274	-0.0640976	0.569904	0.096576	-1637.114519
	Pt(IV)$_{N2}$	-1637.870653	-1637.599573	0.537858	-0.0631975	0.571815	0.097123	-1637.156027
(PtN_3)$_4$ (C_6H_6)	**(PtN_3)$_4$**	-1613.945159	-1613.34442	0.497548	-0.11646504	0.544877	0.126006	-1613.000432
	(PtN_3)$_4$cycloOctyneClickTS	-1925.900653	-1925.205207	0.678575	-0.13829188	0.733991	0.143592	-1924.705714
	(PtN_3)$_4$cycloOctyneProduct	-1926.049509	-1925.367453	0.686608	-0.14454502	0.739804	0.137470	-1924.864299
	Pt(CH_3)$_3$$N_3$	-403.4286385	-403.2755598	0.121835	-0.00873364	0.134056	0.051586	-403.1848001
	Pt(CH_3)$_3$$N_3$cycloOctyneClickTS	-715.4190124	-715.1751089	0.301254	-0.02594437	0.322014	0.07201	-714.9272860
	Pt(CH_3)$_3$$N_3$cycloOctyneProduct	-715.5486168	-715.3209902	0.307045	-0.02779766	0.326108	0.066568	-715.0672805

Table S14. Final Energies, Enthalpy and Entropy Corrections, Gibbs Free Energies from MN15 functional (includes dispersion correction) and SMD solvent correction. In Hartree. See Computational Details for Methods.

Metal (Solvent)	Structure	E(B3LYP/cc-pVDZ)	E(MN15 (SMD)/cc-pVTZ)	ZPE	D0	$H_{correction}$	$S_{correction}$	G
	CycloOctyne (Benzene)	-312.0112817	-311.7046162	0.178609	-0.0155483	0.187449	0.040713	-311.5444449
	CycloOctyne (DMSO)	-312.0112817	-311.7019359	0.178609	-0.0155483	0.187449	0.040713	-311.5417646
	CycloOctyne (THF)	-312.0112817	-311.7041935	0.178609	-0.0155483	0.187449	0.040713	-311.5440222
Au (THF)	**Au-N_3**	-1336.400865	-1335.219183	0.287366	-0.0447659	0.309967	0.079782	-1334.962670
	Au-N_3cycloOctyneClickTS	-1648.390182	-1646.896975	0.466427	-0.0678001	0.497834	0.101566	-1646.467191
	Au_{N1}	-1648.524278	-1647.051565	0.472385	-0.0704289	0.502134	0.095748	-1646.613582
	AuN1toN2isomerizationTS	-1648.500527	-1647.024191	0.471638	-0.0691839	0.502134	0.094948	-1646.585673
	Au_{N2}	-1648.531755	-1647.052979	0.472742	-0.0682811	0.502263	0.097882	-1646.616298
	$AuP(CH_3)_3N_3$	-761.1649753	-760.5297165	0.126565	-0.0135970	0.139606	0.054867	-760.4268714
	$AuP(CH_3)_3N_3$cycloOctyneClickTS	-1073.154266	-1072.207414	0.305784	-0.0363511	0.327519	0.074896	-1071.930076
	$AuP(CH_3)_3N_3$cycloOctyneProduct	-1073.288016	-1072.362008	0.311716	-0.0387612	0.331866	0.070552	-1072.077412
Re (DMSO)	**Re-N_3**	-1078.457350	-1077.508649	0.199196	-0.0408405	0.220220	0.071925	-1077.336619
	Re-N_3cycloOctyneClickTS	-1390.446088	-1389.186366	0.378198	-0.0656304	0.408069	0.094196	-1388.841408
	Re_{N1}	-1390.584551	-1389.339872	0.384948	-0.0686342	0.412937	0.086961	-1388.985199
	ReN1toN2isomerizationTS	-1390.551564	-1389.295581	0.383644	-0.0697456	0.411254	0.086821	-1388.942498
	Re_{N2}	-1390.590465	-1389.341226	0.384732	-0.0645756	0.412875	0.088299	-1388.987511
Ru (C_6H_6)	**Ru-N_3**	-3034.102610	-3031.644069	0.765927	-0.1809022	0.817797	0.138321	-3030.918947
	Ru-N_3cycloOctyneClickTS	-3346.080393	-3343.306304	0.945198	-0.2138496	1.005568	0.157136	-3342.406017
	Ru-N_3cycloOctyneProduct	-3346.193681	-3343.454386	0.951687	-0.2216199	1.010572	0.152519	-3342.546002
	$RuP(CH_3)_3N_3$	-1883.655948	-1882.268854	0.443302	-0.0889423	0.476204	0.093735	-1881.855453
	$RuP(CH_3)_3N_3$cycloOctyneClickTS	-2195.639437	-2193.946415	0.622629	-0.1197783	0.664117	0.112933	-2193.357963
	$RuP(CH_3)_3N_3$cycloOctyneProduct	-2195.764332	-2194.093667	0.629223	-0.1250369	0.669111	0.108089	-2193.496976

Table S14 Cont'd. Final Energies, Enthalpy and Entropy Corrections, Gibbs Free Energies from MN15 functional (includes dispersion correction) and SMD solvent correction. In Hartree. See Computational Details for Methods.

Metal (Solvent)	Structure	E(B3LYP/cc-pVDZ)	E(MN15(SMD)/cc-pVTZ)	ZPE	$H_{correction}$	$S_{correction}$	G
Pt(II) (C_6H_6)	**Pt(II)-N_3**	-1717.690972	-1716.381805	0.618443	0.657461	0.107616	-1715.796447
	Pt(II)-N_3cycloOctyneClickTS	-2029.665348	-2028.051258	0.798756	0.845824	0.124214	-2027.288658
	Pt(II)-N_3cycloOctyneProduct	-2029.802561	-2028.206937	0.805156	0.850693	0.119924	-2027.436593
	Pt(II)P(CH_3)$_3$	-1245.962269	-1245.098357	0.277118	0.300167	0.074648	-1244.848205
	Pt(II)P(CH_3)$_3$$N_3$cycloOctyneClickTS	-1557.949114	-1556.778916	0.456503	0.488118	0.094588	-1556.354172
	Pt(II)P(CH_3)$_3$$N_3$cycloOctyneProduct	-1558.084680	-1556.931636	0.462364	0.492493	0.090608	-1556.499851
W (DMSO)	**W-N_3**	-1071.236245	-1070.288199	0.260776	0.283259	0.073804	-1070.054389
	W-N_3cycloOctyneClickTS	-1382.641196	-1381.967672	0.440151	0.471281	0.093700	-1381.55917
	W_{N1}	-1383.357342	-1382.118006	0.446884	0.476217	0.088260	-1381.700923
	WN1toN2isomerizationTS	-1382.753024	-1382.094587	0.445900	0.474839	0.088250	-1381.678876
	W_{N2}	-1382.781085	-1382.122936	0.446700	0.476169	0.089452	-1381.7067
Pt(IV) (C_6H_6)	**Pt(IV)-N_3**	-1325.737086	-1324.801589	0.352443	0.379196	0.080820	-1324.476542
	Pt(IV)-N_3cycloOctyneClickTS	-1637.722330	-1636.482448	0.531872	0.567109	0.100079	-1635.982392
	Pt(IV)$_{N1}$	-1637.861677	-1636.638174	0.538496	0.572073	0.095106	-1636.129822
	Pt(IV)N1toN2isomerizationTS	-1637.831218	-1636.600388	0.536274	0.569904	0.096576	-1636.09519
	Pt(IV)$_{N2}$	-1637.870653	-1636.64119	0.537858	0.571815	0.097123	-1636.134447
(PtN_3)$_4$ (C_6H_6)	**(PtN_3)$_4$**	-1613.945159	-1612.070135	0.497548	0.544877	0.126006	-1611.609682
	(PtN_3)$_4$cycloOctyneClickTS	-1925.900653	-1923.71596	0.678575	0.733991	0.143592	-1923.078176
	(PtN_3)$_4$cycloOctyneProduct	-1926.049509	-1923.883715	0.686608	0.739804	0.137470	-1923.236016
	Pt(CH_3)$_3$$N_3$	-403.4286385	-402.9381539	0.121835	0.134056	0.051586	-402.8386605
	Pt(CH_3)$_3$$N_3$cycloOctyneClickTS	-715.4190124	-714.6198300	0.301254	0.322014	0.072010	-714.3460627
	Pt(CH_3)$_3$$N_3$cycloOctyneProduct	-715.5486168	-714.7669951	0.307045	0.326108	0.066568	-714.4854877

Table S15. Final Energies, Enthalpy and Entropy Corrections, Gibbs Free Energies from ωB97xD functional (includes dispersion correction) and SMD solvent correction. In Hartree. See Computational Details for Methods.

Metal (Solvent)	Structure	E(B3LYP/cc-pVDZ)	E(ωB97xD (SMD)/cc-pVTZ)	ZPE	D0	$H_{correction}$	$S_{correction}$	G
	CycloOctyne (Benzene)	-312.0112817	-312.016304	0.178609	-0.0155483	0.187449	0.040713	-311.8561327
	CycloOctyne (DMSO)	-312.0112817	-312.0139966	0.178609	-0.0155483	0.187449	0.040713	-311.8538253
	CycloOctyne (THF)	-312.0112817	-312.0161115	0.178609	-0.0155483	0.187449	0.040713	-311.8559402
Au (THF)	**Au-N_3**	-1336.400865	-1336.376668	0.287366	-0.0447659	0.309967	0.079782	-1336.120155
	Au-N_3cycloOctyneClickTS	-1648.390182	-1648.368291	0.466427	-0.0678001	0.497834	0.101566	-1647.938506
	Au_{N1}	-1648.524278	-1648.524698	0.472385	-0.0704289	0.502134	0.095748	-1648.086715
	AuN1toN2isomerizationTS	-1648.500527	-1648.496328	0.471638	-0.0691839	0.502134	0.094948	-1648.057809
	Au_{N2}	-1648.531755	-1648.524462	0.472742	-0.0682811	0.502263	0.097882	-1648.08778
	$AuP(CH_3)_3N_3$	-761.1649753	-761.1911875	0.126565	-0.0135970	0.139606	0.054867	-761.0883424
	$AuP(CH_3)_3N_3$cycloOctyneClickTS	-1073.154266	-1073.182221	0.305784	-0.0363511	0.327519	0.074896	-1072.904882
	$AuP(CH_3)_3N_3$cycloOctyneProduct	-1073.288016	-1073.338793	0.311716	-0.0387612	0.331866	0.070552	-1073.054197
Re (DMSO)	**Re-N_3**	-1078.457350	-1078.426792	0.199196	-0.0408405	0.220220	0.071925	-1078.254762
	Re-N_3cycloOctyneClickTS	-1390.446088	-1390.418368	0.378198	-0.0656304	0.408069	0.094196	-1390.073411
	Re_{N1}	-1390.584551	-1390.57315	0.384948	-0.0686342	0.412937	0.086961	-1390.218477
	ReN1toN2isomerizationTS	-1390.551564	-1390.528453	0.383644	-0.0697456	0.411254	0.086821	-1390.175369
	Re_{N2}	-1390.590465	-1390.573774	0.384732	-0.0645756	0.412875	0.088299	-1390.220059
Ru (C_6H_6)	**Ru-N_3**	-3034.102610	-3034.025997	0.765927	-0.1809022	0.817797	0.138321	-3033.300875
	Ru-N_3cycloOctyneClickTS	-3346.080393	-3346.00311	0.945198	-0.2138496	1.005568	0.157136	-3345.102823
	Ru-N_3cycloOctyneProduct	-3346.193681	-3346.151681	0.951687	-0.2216199	1.010572	0.152519	-3345.243297
	$RuP(CH_3)_3N_3$	-1883.655948	-1883.652508	0.443302	-0.0889423	0.476204	0.093735	-1883.239106
	$RuP(CH_3)_3N_3$cycloOctyneClickTS	-2195.639437	-2195.643566	0.622629	-0.1197783	0.664117	0.112933	-2195.055114
	$RuP(CH_3)_3N_3$cycloOctyneProduct	-2195.764332	-2195.791748	0.629223	-0.1250369	0.669111	0.108089	-2195.195056

Table S15 Cont'd. Final Energies, Enthalpy and Entropy Corrections, Gibbs Free Energies from ωB97xD functional (includes dispersion correction) and SMD solvent correction. In Hartree. See Computational Details for Methods.

Metal (Solvent)	Structure	E(B3LYP/cc-pVDZ)	E(ωB97xD(SMD)/cc-pVTZ)	ZPE	$H_{correction}$	$S_{correction}$	G
Pt(II) (C_6H_6)	**Pt(II)-N_3**	-1717.690972	-1717.797543	0.618443	0.657461	0.107616	-1717.212184
	Pt(II)-N_3cycloOctyneClickTS	-2029.665348	-2029.781254	0.798756	0.845824	0.124214	-2029.018653
	Pt(II)-N_3cycloOctyneProduct	-2029.802561	-2029.939285	0.805156	0.850693	0.119924	-2029.168941
	Pt(II)P(CH_3)$_3$	-1245.962269	-1246.006897	0.277118	0.300167	0.074648	-1245.756745
	Pt(II)P(CH_3)$_3$$N_3$cycloOctyneClickTS	-1557.949114	-1558.00082763	0.456503	0.488118	0.094588	-1557.576084
	Pt(II)P(CH_3)$_3$$N_3$cycloOctyneProduct	-1558.084680	-1558.156063	0.462364	0.492493	0.090608	-1557.724277
W (DMSO)	**W-N_3**	-1071.236245	-1071.223202	0.260776	0.283259	0.073804	-1070.989392
	W-N_3cycloOctyneClickTS	-1382.641196	-1383.214859	0.440151	0.471281	0.093700	-1382.806357
	W_{N1}	-1383.357342	-1383.367703	0.446884	0.476217	0.088260	-1382.95062
	WN1toN2isomerizationTS	-1382.753024	-1383.342891	0.445900	0.474839	0.088250	-1382.951992
	W_{N2}	-1382.781085	-1383.371468	0.446700	0.476169	0.089452	-1382.955232
Pt(IV) (C_6H_6)	**Pt(IV)-N_3**	-1325.737086	-1325.797858	0.352443	0.379196	0.080820	-1325.472811
	Pt(IV)-N_3cycloOctyneClickTS	-1637.722330	-1637.789997	0.531872	0.567109	0.100079	-1637.289941
	Pt(IV)$_{N1}$	-1637.861677	-1637.948366	0.538496	0.572073	0.095106	-1637.440014
	Pt(IV)N1toN2isomerizationTS	-1637.831218	-1637.910983	0.536274	0.569904	0.096576	-1637.405785
	Pt(IV)$_{N2}$	-1637.870653	-1637.950989	0.537858	0.571815	0.097123	-1637.444247
(PtN_3)$_4$ (C_6H_6)	**(PtN_3)$_4$**	-1613.945159	-1614.034769	0.497548	0.544877	0.126006	-1613.574316
	(PtN_3)$_4$cycloOctyneClickTS	-1925.900653	-1925.998404	0.678575	0.733991	0.143592	-1925.36062
	(PtN_3)$_4$cycloOctyneProduct	-1926.049509	-1926.171591	0.686608	0.739804	0.13747	-1925.523891
	Pt(CH_3)$_3$$N_3$	-403.4286385	-403.4294300	0.121835	0.134056	0.051586	-403.3299367
	Pt(CH_3)$_3$$N_3$cycloOctyneClickTS	-715.4190124	-715.4233534	0.301254	0.322014	0.07201	-715.1495861
	Pt(CH_3)$_3$$N_3$cycloOctyneProduct	-715.5486168	-715.5741836	0.307045	0.326108	0.066568	-715.2926762

2.8 Relative Enthalpies and Gibbs Free Energies of SPAAC iClick Reactivity

Table S16. Relative Energies (Becke-Johnson damping corrections, B3LYP/PCM corrected SPE) --Table sorted by metal center; in parentheses is the solvent correction used. All values are in kcal/mol at 298 K and 1 atm.

	Structure	Δ*H*	Δ*G*		Structure	Δ*H*	Δ*G*
Au (THF)	**Au-N_3**	**0.0**	**0.0**	**Pt(II) (C_6H_6)**	**Pt(II)-N_3**	**0.0**	**0.0**
	Au-N_3cycloOctyneClickTS	13.5	21.5		Pt(II)-N3cycloOctyneClickTS	19.9	30.0
	Au_{N1}	-69.2	-58.8		Pt(II)-N3cycloOctyneProduct	-62.4	-50.4
	AuN1toN2isomerizationTS	-51.7	-40.9				
	Au_{N2}	-69.4	-59.9		Pt(II)P(CH_3)$_3N_3$	**0.0**	**0.0**
					Pt(II)P(CH_3)$_3N_3$cycloOctyneClickTS	9.4	18.2
	AuP(CH_3)$_3N_3$	**0.0**	**0.0**		Pt(II)P(CH_3)$_3N_3$cycloOctyneProduct	-73.2	-62.8
	AuP(CH_3)$_3N_3$cycloOctyneClickTS	13.7	22.4	**W (DMSO)**	**W-N_3**	**0.0**	**0.0**
	AuP(CH_3)$_3N_3$cycloOctyneProduct	-69.0	-58.5		W-N_3cycloOctyneClickTS	11.7	20.5
Re (DMSO)	**Re-N_3**	**0.0**	**0.0**		**W_{N1}**	-67.6	-56.5
	Re-N_3cycloOctyneClickTS	12.8	20.6		WN1toN2isomerizationTS	-52.3	-41.2
	Re_{N1}	-68.1	-57.4		**W_{N2}**	-70.2	-59.6
	ReN1toN2isomerizationTS	-49.3	-38.4	**Pt(IV) (C_6H_6)**	**Pt(IV)-N_3**	**0.0**	**0.0**
	Re_{N2}	-69.1	-58.9		Pt(IV)-N_3cycloOctyneClickTS	12.6	21.7
Ru (C_6H_6)	**Ru-N3**	**0.0**	**0.0**		**$Pt(IV)_{N1}$**	-70.3	-59.2
	Ru-N_3cycloOctyneClickTS	20.4	29.6		Pt(IV)N1toN2isomerizationTS	-49.7	-39.2
	Ru-N_3cycloOctyneProduct	-56.4	-45.3		**$Pt(IV)_{N2}$**	-71.8	-61.5
				(PtN_3)$_4$ (C_6H_6)	**(PtN_3)$_4$**	**0.0**	**0.0**
	RuP(CH_3)$_3N_3$	**0.0**	**0.0**		(PtN_3)$_4$cycloOctyneClickTS	30.4	40.1
	RuP(CH_3)$_3N_3$cycloOctyneClickTS	12.1	21.2		(PtN_3)$_4$cycloOctyneProduct	-60.5	-48.2
	RuP(CH_3)$_3N_3$cycloOctyneProduct	-64.4	-53.3				
					Pt(CH_3)$_3N_3$	**0.0**	**0.0**
					Pt(CH_3)$_3N_3$cycloOctyneClickTS	11.7	20.2
					Pt(CH_3)$_3N_3$cycloOctyneProduct	-67.8	-56.9

Table S17. Relative Energies (zero damping corrections, B3LYP/PCM corrected SPE) --Table sorted by metal center; in parenthesis is the solvent correction used. All values are in kcal/mol at 298 K and 1 atm.

	Structure	Δ*H*	Δ*G*		Structure	Δ*H*	Δ*G*
Au (THF)	**Au-N_3**	**0.0**	**0.0**	**Pt (II) (C_6H_6)**	**Pt(II)-N_3**	**0.0**	**0.0**
	Au-N_3cycloOctyneClickTS	14.9	22.9		Pt(II)-N_3cycloOctyneClickTS	19.1	29.2
	Au_{N1}	-67.3	-56.9		Pt(II)-N3cycloOctyneProduct	-63.8	-51.8
	AuN1toN2isomerizationTS	-49.8	-39.0				
	Au_{N2}	-67.7	-58.2		Pt(II)P$(CH_3)_3N_3$	**0.0**	**0.0**
					Pt(II)P$(CH_3)_3N_3$cycloOctyneClickTS	13.0	21.7
	AuP$(CH_3)_3N_3$	**0.0**	**0.0**		Pt(II)P$(CH_3)_3N_3$cycloOctyneProduct	-68.9	-58.5
	AuP$(CH_3)_3N_3$cycloOctyneClickTS	15.2	23.9	**W (C_6H_6)**	**W-N_3**	**0.0**	**0.0**
	AuP$(CH_3)_3N_3$cycloOctyneProduct	-67.2	-56.6		W-N3cycloOctyneClickTS	13.2	21.9
Re (DMSO)	**Re-N_3**	**0.0**	**0.0**		**W_{N1}**	-65.5	-54.4
	Re-N3cycloOctyneClickTS	14.1	21.8		WN1toN2isomerizationTS	-50.0	-39.0
	Re_{N1}	-66.4	-55.6		**W_{N2}**	-67.9	-57.3
	ReN1toN2isomerizationTS	-47.2	-36.4	**Pt (IV) (C_6H_6)**	**Pt(IV)-N_3**	**0.0**	**0.0**
	Re_{N2}	-67.1	-56.9		Pt(IV)-N3cycloOctyneClickTS	14.2	23.2
Ru (C_6H_6)	**Ru-N_3**	**0.0**	**0.0**		**$Pt(IV)_{N1}$**	-68.6	-57.5
	Ru-N_3cycloOctyneClickTS	22.0	31.3		Pt(IV)N1toN2isomerizationTS	-47.6	-37.1
	Ru-N_3cycloOctyneProduct	-53.9	-42.7		**$Pt(IV)_{N2}$**	-70.0	-59.8
				($PtN_3)_4$ (C_6H_6)	**$(PtN_3)_4$**	**0.0**	**0.0**
	RuP$(CH_3)_3N_3$	**0.0**	**0.0**		$(PtN_3)_4$cycloOctyneClickTS	31.3	41.0
	RuP$(CH_3)_3N_3$cycloOctyneClickTS	13.6	22.6		$(PtN_3)_4$cycloOctyneProduct	-59.9	-47.6
	RuP$(CH_3)_3N_3$cycloOctyneProduct	-62.1	-51.1				
					Pt$(CH_3)_3N_3$	**0.0**	**0.0**
					Pt$(CH_3)_3N_3$cycloOctyneClickTS	12.9	21.4
					Pt$(CH_3)_3N_3$cycloOctyneProduct	-66.3	-55.5

Table S18. Relative Energies (zero damping corrections, B3LYP/SMD corrected SPE) --Table sorted by metal center; in parenthesis is the solvent correction used. All values are in kcal/mol at 298 K and 1 atm.

	Structure	Δ*H*	Δ*G*		Structure	Δ*H*	Δ*G*
Au (THF)	**Au-N_3**	**0.0**	**0.0**	**Pt (II) (C_6H_6)**	**Pt(II)-N_3**	**0.0**	**0.0**
	Au-N_3cycloOctyneClickTS	14.7	22.6		Pt(II)-N_3cycloOctyneClickTS	20.0	30.2
	Au_{N1}	-68.7	-58.3		Pt(II)-N3cycloOctyneProduct	-62.7	-50.7
	AuN1toN2isomerizationTS	-51.1	-40.3				
	Au_{N2}	-69.0	-59.5		Pt(II)P$(CH_3)_3N_3$	**0.0**	**0.0**
					Pt(II)P$(CH_3)_3N_3$cycloOctyneClickTS	13.3	22.0
	AuP$(CH_3)_3N_3$	**0.0**	**0.0**		Pt(II)P$(CH_3)_3N_3$cycloOctyneProduct	-69.0	-58.6
	AuP$(CH_3)_3N_3$cycloOctyneClickTS	14.8	23.5	**W (C_6H_6)**	**W-N_3**	**0.0**	**0.0**
	AuP$(CH_3)_3N_3$cycloOctyneProduct	-68.5	-57.9		W-N3cycloOctyneClickTS	12.2	21.0
Re (DMSO)	**Re-N_3**	**0.0**	**0.0**		**W_{N1}**	-67.2	-56.1
	Re-N3cycloOctyneClickTS	12.8	20.6		WN1toN2isomerizationTS	-51.8	-40.7
	Re_{N1}	-68.3	-57.5		**W_{N2}**	-69.7	-59.1
	ReN1toN2isomerizationTS	-49.0	-38.2	**Pt (IV) (C_6H_6)**	**Pt(IV)-N_3**	**0.0**	**0.0**
	Re_{N2}	-68.7	-58.5		Pt(IV)-N3cycloOctyneClickTS	14.3	23.3
Ru (C_6H_6)	**Ru-N_3**	**0.0**	**0.0**		**Pt(IV)$_{N1}$**	-68.7	-57.6
	Ru-N_3cycloOctyneClickTS	22.8	32.0		Pt(IV)N1toN2isomerizationTS	-47.4	-36.9
	Ru-N_3cycloOctyneProduct	-53.0	-41.9		**Pt(IV)$_{N2}$**	-70.8	-60.5
				($PtN_3)_4$ (C_6H_6)	**($PtN_3)_4$**	**0.0**	**0.0**
	RuP$(CH_3)_3N_3$	**0.0**	**0.0**		($PtN_3)_4$cycloOctyneClickTS	32.1	41.9
	RuP$(CH_3)_3N_3$cycloOctyneClickTS	14.3	23.4		($PtN_3)_4$cycloOctyneProduct	-58.8	-46.5
	RuP$(CH_3)_3N_3$cycloOctyneProduct	-61.8	-50.7				
					Pt$(CH_3)_3N_3$	**0.0**	**0.0**
					Pt$(CH_3)_3N_3$cycloOctyneClickTS	12.5	21.1
					Pt$(CH_3)_3N_3$cycloOctyneProduct	-67.3	-56.5

Table S19. Relativ Energies (zero damping corrections, CAM-B3LYP/SMD corrected SPE) --Table sorted by metal center; in parenthesis is the solvent correction used. All values are in kcal/mol at 298 K and 1 atm.

	Structure	Δ*H*	Δ*G*		Structure	Δ*H*	Δ*G*
Au (THF)	**Au-N_3**	**0.0**	**0.0**	**Pt (II) (C_6H_6)**	**Pt(II)-N_3**	**0.0**	**0.0**
	Au-N_3cycloOctyneClickTS	15.6	23.6		Pt(II)-N_3cycloOctyneClickTS	21.4	31.5
	Au_{N1}	-77.4	-67.0		Pt(II)-N3cycloOctyneProduct	-71.0	-59.1
	AuN1toN2isomerizationTS	-59.5	-48.7				
	Au_{N2}	-78.1	-68.6		Pt(II)P(CH_3)$_3N_3$	**0.0**	**0.0**
					Pt(II)P(CH_3)$_3N_3$cycloOctyneClickTS	14.6	23.3
	AuP(CH_3)$_3N_3$	**0.0**	**0.0**		Pt(II)P(CH_3)$_3N_3$cycloOctyneProduct	-77.3	-66.9
	AuP(CH_3)$_3N_3$cycloOctyneClickTS	15.8	24.5	**W (C_6H_6)**	**W-N_3**	**0.0**	**0.0**
	AuP(CH_3)$_3N_3$cycloOctyneProduct	-77.1	-66.6		W-N3cycloOctyneClickTS	13.9	22.7
Re (DMSO)	**Re-N_3**	**0.0**	**0.0**		**W_{N1}**	-76.1	-65.0
	Re-N3cycloOctyneClickTS	13.9	21.7		WN1toN2isomerizationTS	-60.6	-49.5
	Re_{N1}	-77.5	-66.7		**W_{N2}**	-79.0	-68.4
	ReN1toN2isomerizationTS	-56.8	-45.9	**Pt (IV) (C_6H_6)**	**Pt(IV)-N_3**	**0.0**	**0.0**
	Re_{N2}	-78.3	-68.1		Pt(IV)-N3cycloOctyneClickTS	15.5	24.6
Ru (C_6H_6)	**Ru-N_3**	**0.0**	**0.0**		**Pt(IV)$_{N1}$**	-77.7	-66.6
	Ru-N_3cycloOctyneClickTS	24.7	33.9		Pt(IV)N1toN2isomerizationTS	-54.4	-43.9
	Ru-N_3cycloOctyneProduct	-61.0	-49.9		**Pt(IV)$_{N2}$**	-80.2	-70.0
				(PtN_3)$_4$ (C_6H_6)	**(PtN_3)$_4$**	**0.0**	**0.0**
	RuP(CH_3)$_3N_3$	**0.0**	**0.0**		(PtN_3)$_4$cycloOctyneClickTS	36.1	45.8
	RuP(CH_3)$_3N_3$cycloOctyneClickTS	16.2	25.3		(PtN_3)$_4$cycloOctyneProduct	-66.0	-53.7
	RuP(CH_3)$_3N_3$cycloOctyneProduct	-70.0	-59.0				
					Pt(CH_3)$_3N_3$	**0.0**	**0.0**
					Pt(CH_3)$_3N_3$cycloOctyneClickTS	14.0	22.5
					Pt(CH_3)$_3N_3$cycloOctyneProduct	-76.2	-65.4

Table S20. Relative Energies (MN15/SMD corrected SPE) --Table sorted by metal center; in parenthesis is the solvent correction used. All values are in kcal/mol at 298 K and 1 atm.

	Structure	Δ*H*	Δ*G*		Structure	Δ*H*	Δ*G*
Au (THF)	**Au-N_3**	**0.0**	**0.0**	**Pt (II) (C_6H_6)**	**Pt(II)-N_3**	**0.0**	**0.0**
	Au-N_3cycloOctyneClickTS	16.8	24.8		Pt(II)-N_3cycloOctyneClickTS	22.6	32.8
	Au_{N1}	-77.5	-67.1		Pt(II)-N3cycloOctyneProduct	-72.0	-60.1
	AuN1toN2isomerizationTS	-60.3	-49.6				
	Au_{N2}	-78.3	-68.8		Pt(II)P(CH_3)$_3N_3$	**0.0**	**0.0**
					Pt(II)P(CH_3)$_3N_3$cycloOctyneClickTS	15.4	24.1
	AuP(CH_3)$_3N_3$	**0.0**	**0.0**		Pt(II)P(CH_3)$_3N_3$cycloOctyneProduct	-77.7	-67.3
	AuP(CH_3)$_3N_3$cycloOctyneClickTS	16.9	25.6	**W (C_6H_6)**	**W-N_3**	**0.0**	**0.0**
	AuP(CH_3)$_3N_3$cycloOctyneProduct	-77.4	-66.8		W-N3cycloOctyneClickTS	14.5	23.2
Re (DMSO)	**Re-N_3**	**0.0**	**0.0**		**W_{N1}**	-76.8	-65.7
	Re-N3cycloOctyneClickTS	15.4	23.2		WN1toN2isomerizationTS	-63.0	-51.9
	Re_{N1}	-77.8	-67.0		**W_{N2}**	-79.9	-69.4
	ReN1toN2isomerizationTS	-51.1	-40.2	**Pt (IV) (C_6H_6)**	**Pt(IV)-N_3**	**0.0**	**0.0**
	Re_{N2}	-78.7	-68.5		Pt(IV)-N3cycloOctyneClickTS	15.2	24.2
Ru (C_6H_6)	**Ru-N_3**	**0.0**	**0.0**		**Pt(IV)$_{N1}$**	-79.4	-68.3
	Ru-N_3cycloOctyneClickTS	26.8	36.0		Pt(IV)N1toN2isomerizationTS	-57.1	-46.6
	Ru-N_3cycloOctyneProduct	-63.0	-51.8		**Pt(IV)$_{N2}$**	-81.5	-71.2
				(PtN_3)$_4$ (C_6H_6)	**(PtN_3)$_4$**	**0.0**	**0.0**
	RuP(CH_3)$_3N_3$	**0.0**	**0.0**		(PtN_3)$_4$cycloOctyneClickTS	37.9	47.7
	RuP(CH_3)$_3N_3$cycloOctyneClickTS	17.3	26.3		(PtN_3)$_4$cycloOctyneProduct	-63.7	-51.4
	RuP(CH_3)$_3N_3$cycloOctyneProduct	-72.0	-60.9				
					Pt(CH_3)$_3N_3$	**0.0**	**0.0**
					Pt(CH_3)$_3N_3$cycloOctyneClickTS	14.7	23.2
					Pt(CH_3)$_3N_3$cycloOctyneProduct	-75.1	-64.2

Table S21. Relative Energies (ωB97xD/SMD corrected SPE) --Table sorted by metal center; in parenthesis is the solvent correction used. All values are in kcal/mol at 298 K and 1 atm.

	Structure	Δ*H*	Δ*G*		Structure	Δ*H*	Δ*G*
Au (THF)	**Au-N_3**	**0.0**	**0.0**	**Pt (II) (C_6H_6)**	**Pt(II)-N_3**	**0.0**	**0.0**
	Au-N_3cycloOctyneClickTS	15.6	23.6		Pt(II)-N_3cycloOctyneClickTS	21.0	31.2
	Au_{N1}	-79.8	-69.4		Pt(II)-N3cycloOctyneProduct	-75.1	-63.1
	AuN1toN2isomerizationTS	-62.0	-51.3				
	Au_{N2}	-79.6	-70.1		Pt(II)P$(CH_3)_3N_3$	**0.0**	**0.0**
					Pt(II)P$(CH_3)_3N_3$cycloOctyneClickTS	14.4	23.1
	AuP$(CH_3)_3N_3$	**0.0**	**0.0**		Pt(II)P$(CH_3)_3N_3$cycloOctyneProduct	-80.3	-69.9
	AuP$(CH_3)_3N_3$cycloOctyneClickTS	16.0	24.7	**W (C_6H_6)**	**W-N_3**	**0.0**	**0.0**
	AuP$(CH_3)_3N_3$cycloOctyneProduct	-79.5	-69.0		W-N3cycloOctyneClickTS	14.4	23.1
Re (DMSO)	**Re-N_3**	**0.0**	**0.0**		**W_{N1}**	-78.4	-67.4
	Re-N3cycloOctyneClickTS	14.3	22.1		WN1toN2isomerizationTS	-79.3	-68.3
	Re_{N1}	-79.8	-69.0		**W_{N2}**	-80.8	-70.3
	ReN1toN2isomerizationTS	-52.8	-41.9	**Pt (IV) (C_6H_6)**	**Pt(IV)-N_3**	**0.0**	**0.0**
	Re_{N2}	-80.2	-69.9		Pt(IV)-N3cycloOctyneClickTS	15.5	24.5
Ru (C_6H_6)	**Ru-N_3**	**0.0**	**0.0**		**$Pt(IV)_{N1}$**	-80.8	-69.7
	Ru-N_3cycloOctyneClickTS	24.8	34.0		Pt(IV)N1toN2isomerizationTS	-58.7	-48.2
	Ru-N_3cycloOctyneProduct	-65.3	-54.1		**$Pt(IV)_{N2}$**	-82.6	-72.4
				($PtN_3)_4$ (C_6H_6)	**$(PtN_3)_4$**	**0.0**	**0.0**
	RuP$(CH_3)_3N_3$	**0.0**	**0.0**		$(PtN_3)_4$cycloOctyneClickTS	34.1	43.8
	RuP$(CH_3)_3N_3$cycloOctyneClickTS	16.1	25.2		$(PtN_3)_4$cycloOctyneProduct	-70.9	-58.6
	RuP$(CH_3)_3N_3$cycloOctyneProduct	-73.7	-62.6				
					$Pt(CH_3)_3N_3$	**0.0**	**0.0**
					$Pt(CH_3)_3N_3$cycloOctyneClickTS	14.4	22.9
					$Pt(CH_3)_3N_3$cycloOctyneProduct	-77.7	-66.9

2.9 Functional Comparison of $\%V_{bur}$ vs. $\Delta G^{\ddagger}$

Table S22. Comparison of Different Functionals' Calculated Enthalpic and Gibb's Free Energy Barriers for SPAAC iClick ($\Delta H^{\ddagger}$ and $\Delta G^{\ddagger}$)

	B3LYP (PCM)		B3LYP (SMD)		CAM-B3LYP (SMD)		MN15 (SMD)		ωB97xD (SMD)	
Compound	$\Delta H^{\ddagger}$	$\Delta G^{\ddagger}$	$\Delta H^{\ddagger}$	$\Delta G^{\ddagger}$	$\Delta H^{\ddagger}$	$\Delta G^{\ddagger}$	$\Delta H^{\ddagger}$	$\Delta G^{\ddagger}$	$\Delta H^{\ddagger}$	$\Delta G^{\ddagger}$
Au-N_3	14.9	22.9	14.7	22.6	14.3	22.3	16.8	24.8	15.6	23.6
Au$P(CH_3)_3N_3$	15.2	23.9	14.8	23.5	14.5	23.2	16.9	25.6	16.0	24.7
Re-N_3	14.1	21.8	12.8	20.6	12.4	20.2	15.4	23.2	14.3	22.1
Ru-N_3	22.0	31.3	22.8	32.0	21.8	31.0	26.8	36.0	24.8	34.0
Ru$P(CH_3)_3N_3$	13.6	22.6	14.3	23.4	13.6	22.6	17.3	26.3	16.1	25.2
Pt(II)-N_3	19.1	29.2	20.0	30.2	18.7	28.9	22.6	32.8	21.0	31.2
Pt(II)$P(CH_3)_3N_3$	13.0	21.7	13.3	22.0	12.3	21.0	15.4	24.1	14.4	23.1
W-N_3	13.2	21.9	12.2	21.0	11.6	20.3	14.5	23.2	14.4	23.1
Pt(IV)-N_3	14.2	23.2	14.3	23.3	13.3	22.3	15.2	24.2	15.5	24.5
$(PtN_3)_4$	31.3	41.0	32.1	41.9	34.0	43.8	37.9	47.7	34.1	43.8
Pt$(CH_3)_3N_3$	12.9	21.4	12.5	21.1	12.3	20.8	14.7	23.2	14.4	22.9

*****Highlighted azides were attempted experimentally.

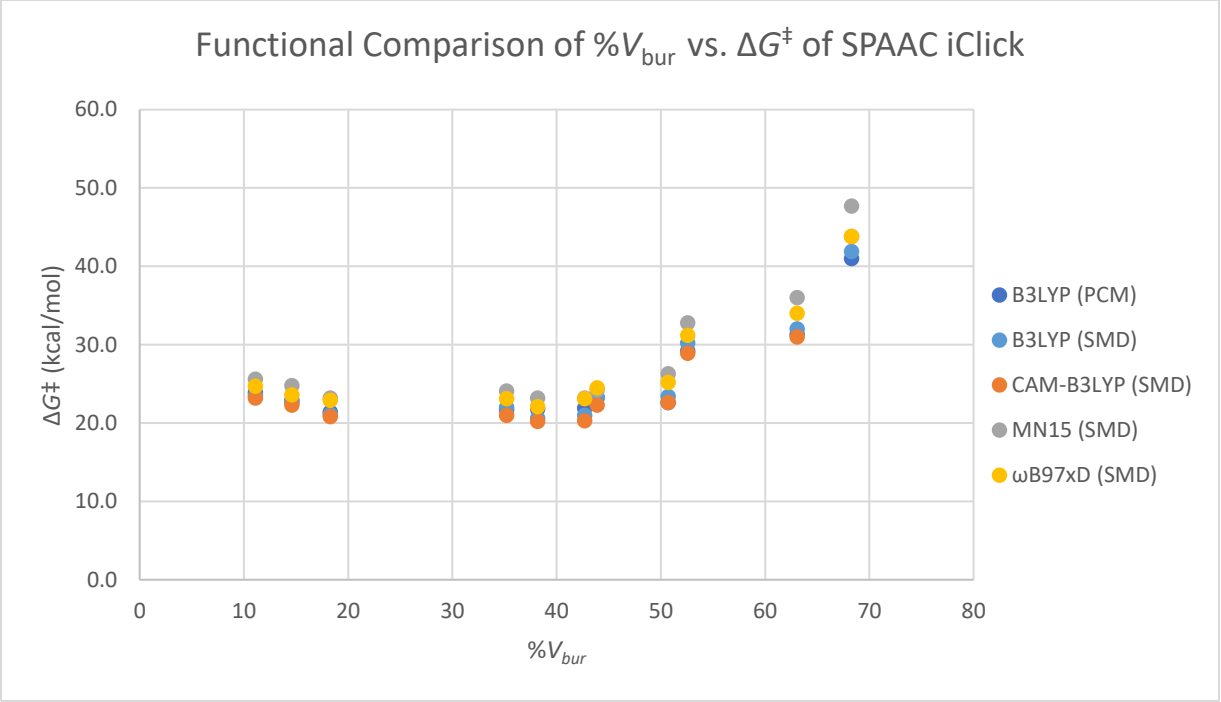

Figure S31. %V_{bur} vs. $\Delta G^{\ddagger}$ for the various theoretical functionals analyzed. All functionals illustrate the same general trend; that the $\Delta G^{\ddagger}$ is directly affected by %V_{bur}. This effect is "turned on" as %V_{bur} increases above 50%.

2.10 Effect of Solvent optimization on **Au-N_3** Energies

Table S23. Au-N_3 Energies, Enthalpy and Entropy Corrections, Gibbs Free Energies with Solvent Optimization Correction-structures optimized with solvent correction (THF) at both optimization and single-point energy calculations (zero damping dispersion correction, D0, used).

Structures (THF)	E(B3LYP/cc-pVDZ)	E(B3LYP/cc-pVTZ)	ZPE	D0	$H_{correction}$	$S_{correction}$	*G*
Cyclooctyne	-312.013	-312.1151182	0.178392	-0.0155411	0.187240	0.0407140	-311.971
Au-N_3	-1336.42	-1336.680816	0.287179	-0.0447322	0.309839	0.079997	-1336.47
Au-N_3cycloOctyneClickTS	-1648.40	-1648.764873	0.465916	-0.0678064	0.497386	0.101549	-1648.40
Au_{N1}	-1648.54	-1648.898010	0.472341	-0.0705372	0.502093	0.095916	-1648.53
AuN1toN2isomerizationTS	-1648.52	-1648.871044	0.471455	-0.0691844	0.500681	0.095171	-1648.50
Au_{N2}	-1648.55	-1648.90078	0.472435	-0.0682111	0.501293	0.092646	-1648.53

Table S24. Effect of Solvent on **Au-N_3** Potential Energy Surface -structures optimized with solvent correction (THF) at both optimization and single-point energy calculations (zero damping dispersion correction, D0, used).

Structure (THF)	Δ*H*	Δ*G*
Au-N_3	**0.0**	**0.0**
Au-N_3cycloOctyneClickTS	15.0	23.0
Au_{N1}	-67.3	-56.9
AuN1toN2isomerizationTS	-50.5	-39.7
Au_{N2}	-68.1	-56.3

3. References

1 G. M. Sheldrick, *Acta Cryst.*, 2015, **C71**, 3–8.
2 S. Vailati Facchini, J. M. Neudörfl, L. Pignataro, M. Cettolin, C. Gennari, A. Berkessel and U. Piarulli, *ChemCatChem*, 2017, **9**, 1461–1468.
3 H. C. Kolb, M. G. Finn and K. B. Sharpless, *Angew. Chem. Int. Ed.*, 2001, **40**, 2004–2021.
4 P. Schmid, M. Maier, H. Pfeiffer, A. Belz, L. Henry, A. Friedrich, F. Schönfeld, K. Edkins and U. Schatzschneider, *Dalton Trans.*, 2017, **46**, 13386–13396.
5 K. S. Schanze, D. Brent MacQueen, T. A. Perkins and L. A. Cabana, *Coord. Chem. Rev.*, 1993, **122**, 63–89.
6 C. K. Chen, H. C. Tong, C. Y. C. Hsu, C. Y. Lee, Y. H. Fong, Y. S. Chuang, Y. H. Lo, Y. C. Lin and Y. Wang, *Organometallics*, 2009, **28**, 3358–3368.
7 K. H. von Dahlen and J. Lorberth, *J. Organomet. Chem.*, 1974, **65**, 267–273.
8 S. Schlecht, N. Faza, W. Massa, S. Dapprich, G. Frenking and K. Dehnicke, *Z. Anorg. Allg. Chem.*, 1998, **624**, 1011–1014.
9 M. J. Frisch, G. W. Trucks, H. B. Schlegel, G. E. Scuseria, M. A. Robb, J. R. Cheeseman, G. Scalmani, V. Barone, B. Mennucci, G. A. Petersson, H. Nakatsuji, M. Caricato, X. Li, H. P. Hratchian, A. F. Izmaylov, J. Bloino, G. Zheng, J. L. Sonnenberg, M. Hada, M. Ehara, K. Toyota, R. Fukuda, J. Hasegawa, M. Ishida, T. Nakajima, Y. Honda, O. Kitao, H. Nakai, T. Vreven, J. A. Montgomery Jr., J. E. Peralta, F. Ogliaro, M. Bearpark, J. J. Heyd, E. Brothers, K. N. Kudin, V. N. Staroverov, R. Kobayashi, J. Normand, K. Raghavachari, A. Rendell, J. C. Burant, S. S. Iyengar, J. Tomasi, M. Cossi, N. Rega, J. M. Millam, M. Klene, J. E. Knox, J. B. Cross, V. Bakken, C. Adamo, J. Jaramillo, R. Gomperts, R. E. Stratmann, O. Yazyev, A. J. Austin, R. Cammi, C. Pomelli, J. W. Ochterski, R. L. Martin, K. Morokuma, V. G. Zakrzewski, G. A. Voth, P. Salvador, J. J. Dannenberg, S. Dapprich, A. D. Daniels. Farkas, J. B. Foresman, J. V Ortiz, J. Cioslowski and D. J. Fox, *Gaussian 09 Revis. C.01*, 2010, Gaussian Inc., Wallingford CT.
10 A. D. Becke, *J. Chem. Phys.*, 1993, **98**, 5648–5652.
11 C. Lee, W. Yang and R. G. Parr, *Phys. Rev. B*, 1988, **37**, 785-789.
12 N. B. Balabanov and K. A. Peterson, *J. Chem. Phys.*, 2005, **123**, 64107.
13 N. B. Balabanov and K. A. Peterson, *J. Chem. Phys.*, 2006, **125**, 074110.
14 K. L. Schuchardt, B. T. Didier, T. Elsethagen, L. Sun, V. Gurumoorthi, J. Chase, J. Li and T. L. Windus, *J. Chem. Inf. Model.*, 2007, **47**, 1045–1052.
15 E. J. Baerends, D. E. Ellis and P. Ros, *Chem. Phys.*, 1973, **2**, 41–51.
16 J. L. Whitten, *J. Chem. Phys.*, 1973, **58**, 4496–4501.
17 M. Feyereisen, G. Fitzgerald and A. Komornicki, *Chem. Phys. Lett.*, 1993, **208**, 359–363.
18 O. Vahtras, J. Almlöf and M. W. Feyereisen, *Chem. Phys. Lett.*, 1993, **213**, 514–518.
19 H. P. Hratchian and H. B. Schlegel, *J. Chem. Theory Comput.*, 2005, **1**, 61–69.
20 J. Tomasi, *Theor. Chem. Acc.*, 2004, **112**, 184–203.
21 S. Grimme, *Wiley Interdiscip. Rev. Comput. Mol. Sci.*, 2011, **1**, 211–228.
22 S. Grimme, S. Ehrlich and L. Goerigk, *J. Comput. Chem.*, 2011, **32**, 1456–1465.
23 S. Tobisch and T. Ziegler, *J. Am. Chem. Soc.*, 2004, **126**, 9059–9071.
24 F. Zaccaria, C. Ehm, P. H. M. Budzelaar and V. Busico, *ACS Catal.*, 2017, **7**, 1512–1519.
25 F. Zaccaria, R. Cipullo, P. H. M. Budzelaar, V. Busico and C. Ehm, *J. Polym. Sci. Part A Polym. Chem.*, 2017, **55**, 2807–2814.
26 A. V. Marenich, C. J. Cramer and D. G. Truhlar, *J. Phys. Chem. B*, 2009, **113**, 6378–6396.
27 T. Yanai, D. P. Tew and N. C. Handy, *Chem. Phys. Lett.*, 2004, **393**, 51–57.
28 H. S. Yu, X. He, S. L. Li and D. G. Truhlar, *Chem. Sci.*, 2016, **7**, 5032–5051.
29 M. J. Frisch, G. W. Trucks, H. B. Schlegel, G. E. Scuseria, M. A. Robb, J. R. Cheeseman, G. Scalmani, V. Barone, G. A. Petersson, H. Nakatsuji, X. Li, M. Caricato, A. V. Marenich, J. Bloino, B. G. Janesko, R. Gomperts, B. Mennucci, H. P. Hratchian, J. V. Ortiz, A. F. Izmaylov, J. L. Sonnenberg, D. Williams-Young, F. Ding, F. Lipparini, F. Egidi, J. Goings, B. Peng, A. Petrone, T. Henderson, D. Ranasinghe, V. G. Zakrzewski, J. Gao, N. Rega, G. Zheng, W. Liang, M. Hada, M. Ehara, K. Toyota, R. Fukuda, J. Hasegawa, M. Ishida, T. Nakajima, Y. Honda, O. Kitao, H. Nakai, T. Vreven, K. Throssell, J. Montgomery, J. A., J. E. Peralta, F. Ogliaro, M. J. Bearpark, J. J. Heyd,

E. N. Brothers, K. N. Kudin, V. N. Staroverov, T. A. Keith, R. Kobayashi, J. Normand, K. Raghavachari, A. P. Rendell, J. C. Burant, S. S. Iyengar, J. Tomasi, M. Cossi, J. M. Millam, M. Klene, C. Adamo, R. Cammi, J. W. Ochterski, R. L. Martin, K. Morokuma, O. Farkas, J. B. Foresman and D. J. Fox, *Gaussian 16 Revis. C.01, 2016, Gaussian, Inc., Wallingford, CT*.

30 J. Da Chai and M. Head-Gordon, *Phys. Chem. Chem. Phys.*, 2008, **10**, 6615–6620.

31 L. Falivene, R. Credendino, A. Poater, A. Petta, L. Serra, R. Oliva, V. Scarano and L. Cavallo, *Organometallics*, 2016, **35**, 2286–2293.